1-1-2016

Coupled and Uncoupled Earth Pressure Profiles in Unsaturated Soils under Transient Flow

Syed Gous Andrabi

Coupled and uncoupled earth pressure profiles in unsaturated soils under transient flow

By

Syed Gous Andrabi

A Thesis
Submitted to the Faculty of
Mississippi State University
in Partial Fulfillment of the Requirements
for the Degree of Master of Science
in Civil Engineering
in the Department of Civil and Environmental Engineering

Mississippi State, Mississippi

December 2016

Coupled and uncoupled earth pressure profiles in unsaturated soils under transient flow

By

Syed Gous Andrabi

Approved:

_____

Farshid Vahedifard
(Major Professor)

_____

Shantia Yarahmadian
(Committee Member)

_____

John F. Peters
(Committee Member)

_____

James L. Martin
(Graduate Coordinator)

_____

Jason M. Keith
Dean
Bagley College of Engineering

Name: Syed Gous Andrabi

Date of Degree: December 9, 2016

Institution: Mississippi State University

Major Field: Civil Engineering

Major Professor: Dr. Farshid Vahedifard

Title of Study: Coupled and uncoupled earth pressure profiles in unsaturated soils under transient flow

Pages in Study 68

Candidate for Degree of Master of Science

The main goal of this research is to evaluate the behavior of earth pressure profiles in unsaturated soils under transient flow. In the first part, an empirical correlation is proposed to obtain the fitting parameters of Brooks and Corey's soil-water retention model from Fredlund and Xing's model. The retention models and the proposed equivalency between the models were assessed for 601 soil samples from the unsaturated soils hydraulic database (UNSODA). In the second part, a coupled one-dimensional hydro-mechanical model is introduced and is implemented into Rankine's earth-pressure model to represent active and passive earth pressure profiles in unsaturated soils under transient flow. A realistic coupling process of infiltration and deformation in the porous medium is established based on the variation in permeability along with deformation in the soil body. The results showed that ignoring the hydro-mechanical coupling effect can lead to underestimation of earth pressure values, especially for fine-grained soils.

DEDICATION

I dedicate this work to my parents, Nisar Ahmad Andrabi and Kaunsar Andrabi, who persuaded me to embark on the high road of knowledge in pursuit of my academic ambitions in an unbeknown foreign land. Were it not for their prudent vision, uncompromising resolve for excellent education, and unwavering trust in my abilities, these words would never have been inked. This work is a fulfilling fruition to their innumerable prayers

ACKNOWLEDGEMENTS

I would like to express my sincere appreciation to several people who have contributed to the development and accomplishment of this research. Most importantly, I feel obliged to express my deepest gratitude to my advisor, Dr. Farshid Vahedifard, for his constant guidance, supervision, encouragement, and financial assistance.

I would also like to thank my committee members, Dr. Shantia Yarahmadian and Dr. John F. Peters, for their insightful comments and guidance throughout my research. I am grateful to Dr. Shantia Yarahmadian for his patience, guidance and help in solving many complex mathematical problems related to my research.

I would like to thank all my colleagues Clay, Firas, James, Jody, Jonathan, Kimia, Mohammad, and Shahriar for their help and guidance. Also, I am very thankful to all of my friends in Starkville for their kind support and help.

Finally, I would like to thank my parents and younger brothers for their encouragement, patience, and support throughout the course of my studies.

TABLE OF CONTENTS

LIST OF TABLES

LIST OF FIGURES

CHAPTER I

INTRODUCTION

1.1 Background

The flow in unsaturated porous media has gained much attention over the recent years because of its association with many geotechnical problems. In unsaturated soil mechanics, the negative pore water pressure in the vadose zone is a function of precipitation intensity, duration and deformation interaction (Wu et al., 2011; Wu et al., 2013; Wu et al., 2015; Wu et al., 2016). This dynamic process may alter the stress profiles or the lateral earth pressure profiles, which might lead to various infrastructural failures, or at least the poor performance of, retaining walls, basement walls, pile foundations, tunnels, and sewers.

Many Geo-structures are usually designed and analyzed based on the hypothetical stress profiles in soil. Several key aspects contribute to different profiles of matric suction corresponding to the depth in an unsaturated porous media. The most important aspects are the hydrologic properties of the soil which can be estimated from the hydraulic conductivity function (HCF) and the soil water retention curve (SWRC). The SWRC's are usually estimated from the experimental measurements and a subsequent fitting of a parametric model to measured data. The fitting parameters of one model can also be predicted from another by developing an equivalence between them by using empirical, numerical or analytical techniques. Although, some SWR functions are highly non- linear

and cannot be solved analytically such as Fredlund and Xing (1994), however, the parameters of such models can be converted to simpler models like Brooks and Corey (1964), which can be easily solved both numerically and analytically.

The hydrological properties from the retention functions for different unsaturated soils can be used in transient flow analysis to study the profiles of matric suction, or lateral earth pressure. However, several other aspects like precipitation and evaporation, which are dependent on time, also contribute to the different profiles of matric suction. The precipitation rate is inversely related to the matric suction and directly related to the moisture content as increase in precipitation will decrease the matric suction and increase the moisture content. Alternatively, increasing evaporation rate will increase matric suction and decrease moisture content. The transient analysis of infiltration in unsaturated soils is more illustrative than the much simpler steady state analysis because of the change in surface boundary conditions and the degree of saturation with time. The role of matric suction is not commonly considered in the design of earth retaining structures, due to complexities and uncertainties associated with reliable determination of matric suction value during the life span of the structure. However, incorporating unsaturated flow characteristic into lateral earth pressure profile will allow us to better understand the performance of earth retaining systems and also, can be used for back-analysis purposes.

1.2 Objective

The primary objective of this research is to investigate profiles of earth pressures in unsaturated soils under transient flow, using the coupled infiltration and deformation equations of one dimensional flow, and comparing them with uncoupled one dimensional flow. An ancillary objective is to investigate the correspondence of fitting parameters of

well-known SWRCs proposed by Brooks and Corey (1964) and Fredlund and Xing (1994).

1.3 Scope

The first task of this research was to investigate the correlation between two of most commonly used retention functions. In this part of the study, an empirical correlation is proposed to estimate the fitting parameter (λ) used in the Brooks and Corey (1964) (BC) model from Fredlund and Xing (1994) (FX) fitting parameters(n, m). The parameters for BC's retention function can be obtained by fitting the nonlinear function directly to the measured data or by converting to equivalent FX parameters by means of an empirical approach. To describe soil water retention curve more accurately and over a wider range of matric suction, BC model parameters can be estimated by developing a correlation with Fredlund & Xing (FX) function, which provides a steadier and continuous retention model. Both the BC and FX models were assessed using 601 samples from the unsaturated soils hydraulic database (UNSODA), whereby each sample was analyzed for unsaturated soil hydraulic properties and retention curves. Distinctive fitting parameters were estimated for each soil water retention function by the constrained nonlinear optimization method. Moreover, the BC model parameters were also evaluated using the proposed relation using FX parameters, the converted parameters were used in BC's function to generate the SWRC. Finally, the actual BC's retention curve is compared with the one generated from the converted parameters.

The second task of this research was to develop a coupled hydro-mechanical model to simulate lateral earth pressure profiles in unsaturated soils under transient flow. To accomplish this task, a one-dimensional coupled hydro-mechanical model is

developed based on the coupled infiltration and deformation governing equations. The coupled model along with a unified effective stress approach are then implemented into Rankine's earth pressure theory to study the profiles of active and passive lateral earth pressures. The governing equations for coupled/uncoupled infiltration under transient flow were derived based on Darcy's law, mass conservation, Gardner's HCF and SWR function, Hook's law and unified effective stress approach. Variations in the degree of saturation in transient flow significantly influences the matric suction, suction stress, and effective stress. The changes in effective stress is central to the study of lateral earth pressures that occur over time. The variation in permeability along with deformation in the soil body enables one to establish a realistic coupling process of seepage and deformation in the permeable medium. Variations in permeability are associated with stress state during the infiltration while the deformation is expressed based on the principle of effective stress.

CHAPTER II

EMPIRICAL EQUIVALENCE OF THE FITTING PARAMETERS OF SOIL WATER RETENTION MODELS

2.1 Introduction

Many studies related to the vadose zone flow and transport are based on soil hydraulic properties. To quantify these properties, the SWRC, which relates the water pressure head to volumetric water content, is requisite. SWRC's are generally determined from the laboratory measurements and consequent fitting of a parametric model to measured data. Most of the works related to the development of the soil water retention models are based on the integral equations given by Burdine (1953) or Mualem (1976), along with the fractal behavior (Cihan et al., 2009). Several empirical equations like Gardner (1958), Brooks and Corey (1962) and statistical models like van Genuchten (1980), Fredlund and Xing (1994) have been proposed to define the SWRC. However, estimation of the parameters in these models remains challenging and inefficient. Several methods (e.g., van Genuchten, 1980; Philip, 1985; Lenhard et al., 1989; Warrick, 1995; Morel-Seytoux et al., 1996; Fredlund et al., 2002; Haverkamp et al., 2005; Leij et al., 2005) have been developed to establish equivalency between the models in order to predict the parameters of one model from another.

Most of the studies that have been done on parameter equivalence or correspondence usually ensure that either the capillary drive (Morel-Seytoux et al., 1996)

or capillary length (Warrick 1995), which represents the total energy, is preserved (Rucker et al., 2005) or attempt to find the parameters that minimize the dissimilarities among the retention curves (Lenhard et al., 1989, Rucker et al., 2005). The most recent approach, which involves the equivalence of shape parameters, was introduced by Haverkamp et al. (2005). This approach overcomes the major issues with changing over parameters of various retention functions by describing the retention conduct of a specific soil with a solitary number, the shape index. The shape index (P), in terms of shape parameters, ascertains the inflection point and the slope of the SWRC, and can be accordingly rendered as the mean slope about the inflection point (Haverkamp et al., 2005). The most commonly used and the simplest form of conversion approach is least square optimization, which estimates the fitting parameters of one function using the known parameters of the other function by minimizing the differences between the two functions. However, the least square optimization approach does not yield any derivation of the correspondence equation between two functions (Ghezzehei et al., 2007).

While BC's simple functional form provides a convenient model for implementation in analytical solutions, the BC model cannot reasonably represent the soil behavior over a wide range of suction. Further, the BC function has substantial complications with direct fitting to the measured data for fine-textured soils near saturation (van Genuchten and Nielsen, 1985; Milly, 1987). Also, due to lack of inflection point in the BC function, the relationship may result in inaccuracies between laboratory and field measurements. Moreover, the discontinuity in the primary derivative at the air entry value causes some problems in fitting BC parameters directly to the measured data (Milly, 1987). To overcome such problems, the data can be fitted to FX's

model, which does not have the same pathological behavior as BC, and provides a realistically better inherent fit for the measured data (Fredlund and Xing, 1994). The parameters obtained by fitting the data to FX can be correlated to the fitting parameters of BC. Although, the model prediction as a result of conversion could vary considerably due to the divergence of transformed parameters. Distribution of the parameters amid the SWR functions permits the extrapolation of one function if the other is known (Cihan et al., 2009). The reason for estimating BC from other functions is that the BC's function is very simple with fewer fitting parameters and can be solved easily both numerically and analytically provided the aforementioned technical problems can be avoided.

The main objective of this study is to propose an approach to estimate the BC's fitting parameter (λ) using the parameters (m, n) of FX's retention model. The retention models are fitted with the measured data to generate the respective SWRC's. The fitting parameters of BC (θ_s, h_a, λ) and FX (θ_s, a, n, m) are calculated by constrained non-linear optimization. An empirical correlation is proposed that estimates the BC's parameter from the FX's parameters. Different parameters from each retention function are compared to investigate any correlation. The converted parameters are used in BC's function to generate the SWRC. Finally, the actual BC's retention curve is compared with the one generated from the converted parameters.

2.2 Unsaturated soil hydraulic database

In this study, the unsaturated soil hydraulic database (UNSODA) (Leij et al. 1996) was used for evaluating the BC and FX models and also, to establish the equivalency correlation between the two models. The UNSODA includes a wide variety and range of retention and conductivity data that can be implemented in research and engineering

applications involving the vadose zone. The data in the UNSODA were collected from the literature and also was requested from engineers and scientists around the world. The UNSODA consists of parameters quantifying hydraulic properties for 780 unsaturated soils including hydraulic conductivity, water retention, etc. It also includes basic soil properties such as particle size distribution, organic matter content, porosity, bulk density, etc., as well as the information about the experimental procedures.

The soils in the UNSODA are classified on the basis of texture ranging from clay to sand, and in total it is comprised of data for 12 types of soils. Due to differences in the conceptions and the procedures adopted to obtain the data, there is an extensive variability in its quantity and quality. For example, different methods were adopted for the measurement of volumetric water content data, which results in a difference from one data set to other with different accuracies. The current study considers a total of 601 soil samples from 10 different soil textures. Sandy clay and silt textured soils were excluded because of inadequate data. Also, in each soil texture, only the soils with five or more data sets were considered; soils with muddled or fewer data sets were ignored. Every individual soil sample is represented by a code, since some experimental tests generate a lot of identical data. To keep the size of database sensible, and also to avoid the repetition of the data, each soil samples is defined with a numeric code or identifier (Leij et al., 1996). Figure 2.1 shows the number of soils for 10 different textures from UNSODA considered in this study.

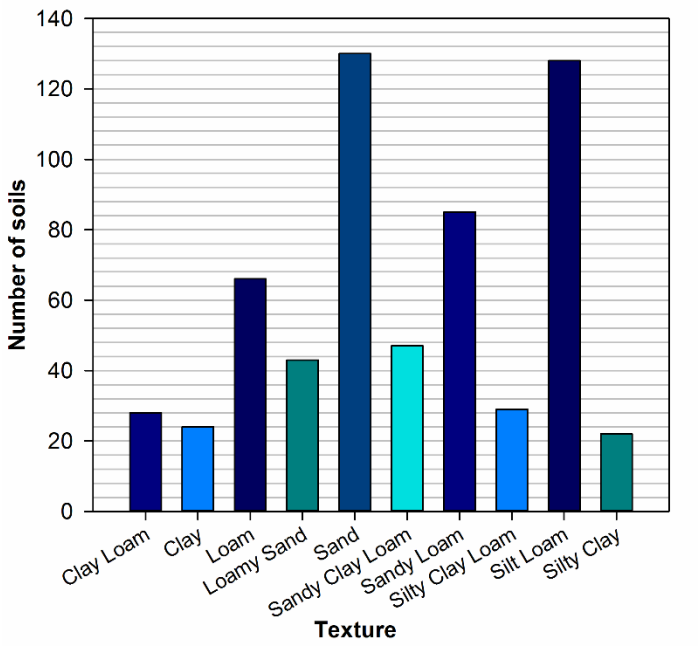

Figure 2.1 Number of soils considered in this study from UNSODA, classified based on texture

2.3 Theory

2.3.1 Soil water retention curve functions

SWRC is an imperatively distinctive property of flow in unsaturated soil regions. To measure the flow and distribution of water in unsaturated soils, it is necessary to have an understanding of SWRC. Measured SWRC data are used to estimate parameters for different models by fitting the nonlinear functions directly to the measured data. Experimental measurement of SWRC is very complex and time-consuming. For classification and collation among different soil types and situations, or for analysis and modeling purposes, it is recommended to represent the SWRC as a mathematically continuous function. A few methodologies, extending from experimental parametric expressions to physically based models with parameters determined from quantifiable

medium properties, can be used to identify a persistent soil water characteristic curve. Various functions have been recommended for depicting the SWRC but in this study, two well-known parametric models will be discussed and are further explained below:

2.3.1.1 Brooks and Corey (1964)

BC suggested an equation for SWRC for representing soil suction in two different zones based on the values of soil suction greater or lesser than air entry value. The equation is given as:

$$\frac{\theta-\theta_r}{\theta_s-\theta_r} = \begin{cases} \left(\frac{h}{h_a}\right)^{-\lambda} & for\ h > h_a \\ 1 & for\ 0 \le h \le h_a \end{cases} \quad (2.1)$$

where θ, θ_s and θ_r represent volumetric water content, saturated water content and residual water content, respectively, h_a represents the bubbling pressure, also known as air entry value, h is the matric suction head and λ is the parameter for the pore size distribution index (Brooks and Corey, 1964). This equation has two fitting parameters (h_a and λ) and one empirical parameter (θ_r) . Hypothetically, the value of λ tends to reach a lower bound of zero for the soils having a very large range of pore sizes. Alternatively, for evenly distributed pore sizes, λ tends towards infinity (Kosugi et al., 2002). The principle inadequacies of BC model are, firstly, the derivative at h_a is discontinuous, and, secondly, the nonappearance of an inflection point, which may bring about the errors with field-measured data (Milly, 1987; Assouline and Tartakovsky, 2001).

In this study, the residual water content is not considered as a fitting parameter ($\theta_r = 0$), the BC function can be represented as:

$$\frac{\theta}{\theta_s} = \begin{cases} \left(\frac{h}{h_a}\right)^{-\lambda} & for\ h > h_a \\ 1 & for\ 0 \leq h \leq h_a \end{cases} \tag{2.2}$$

2.3.1.2 Fredlund and Xing (1994)

Fredlund and Xing (1994) suggested an equation for the SWRC for matric suction values ranging from 0 to 1.0 x10^6 kPa.

$$\frac{\theta}{\theta_s} = C(h)\frac{1}{\left\{ln\left[e+\left(\frac{h}{a}\right)^n\right]\right\}^m} \tag{2.3}$$

where e is Euler's constant, a is defined as the approximate air entry value of the soil, n is defined as a factor that controls the slope at the point of inflection in the SWRC, m is a parameter that corresponds to the curvature of the FX in the high matric suction range. The correction factor $C(h)$ extends the suction range to entirely dry conditions past residual suction i.e., at maximum matric suction (1×10^6), the water content is zero. The correction factor is given by:

$$C(h) = 1 - \frac{ln\left(1+\frac{h}{C_r}\right)}{ln\left(1+\frac{1000000}{C_r}\right)} \tag{2.4}$$

where h is any soil suction, C_r is a constant identified with h (matric suction) corresponding to θ_r. A constant value for C_r can be assumed for most of the soils. The value for C_r can be determined by localizing a point where the curve begins to drop linearly in the high suction range.

The FX function has four fitting parameters (θ_s, a, n, m) and θ_r is considered zero (Fredlund and Xing, 1994). Leong and Rahardjo (1997) concluded that FX's function describes the SWRC more precisely than any other retention function (Gardner, 1958; Brooks and Corey, 1964; van Genuchten, 1980) over the wide range of suction. The van

Genuchten (vG) function is considered to fit data well as compared to the other methods. The problem with vG is that it falls rapidly in the direction of zero water content for an exceptionally narrow range of matric suctions, and is not reasonable in the high matric suction range (Lamara and Derriche, 2008; Rahardjo and Leong, 1997). Whereas, FX's function drops more gradually with the increase in matric suction and offers a realistically continuous fit for the experimental data in the entire suction range ($0 - 1.0 \times 10^6$kPa) (Fredlund and Xing, 1994).

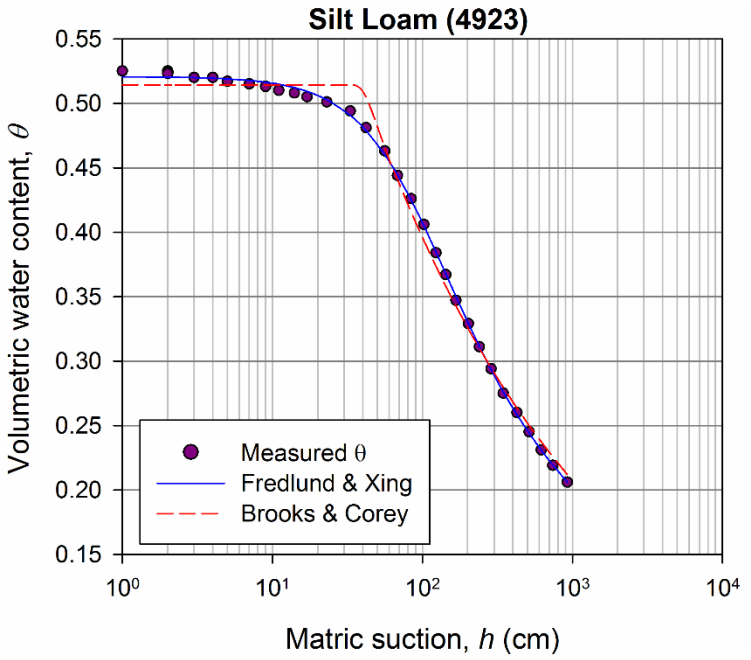

Figure 2.2 SWRC's of Brooks & Corey and Fredlund & Xing retention functions

Brooks & Corey and Fredlund & Xing parametric models fitted to measured data of silt loam (4923) from UNSODA

Figure 2.2 shows SWRC for silt loam soil and the number in the parenthesis (4923) represents the identification code used in UNSODA for a specific soil. In Figure 2.2, the experimental data points are fitted by the BC and FX retention models. The

models fit the data well except there is a discontinuity when matric suction is equal to air entry value in case of BC, which is the most prominent difference between BC and FX. The subsequent fitting parameters for the BC model are: $\theta_s = 0.514\ \mathrm{cm}^3/\mathrm{cm}^3$; $\mathrm{h_a} = 39.35$ cm; and $\lambda = 0.281$. While, the fitting parameters for FX are: $\theta_s = 0.521\ \mathrm{cm}^3/\mathrm{cm}^3$; $a = 74.122$ cm; $n = 1.595$; $m = 0.631$ and $C_r = 3689.5$.

2.3.2 Investigated conversion methods

In this study, different conversion approaches were studied to find the correspondence of BC's retention model with the FX. Some of the studied approaches are briefly discussed as follows: Capillary Length was defined by Philip (1985) and Warrick (1995). To preserve the capillary length, the definition of the restraints (matric suction range) for the evaluation of the water retention function is necessary. The matric suction range usually lies between the matric suction at wetting and the matric suction at drying fronts and typically depends on the particular problem (Rucker et al., 2005). Effective Capillary drive (Morel-Seytoux et al., 1996) is well-defined as an integral measure of the relative hydraulic conductivity. In fact, the capillary drive is a modified capillary length approach, for which the matric suction at wetting is 0 and the matric suction at drying tends to negative infinity. The capillary length and the capillary drive approaches involve the estimation of the respective capillary length or capillary drive for both the BC and FX functions and then matching them together so that the capillary length or the effective capillary drive is preserved, thus defining a correlation between the two functions.

Another conversion approach, proposed by Haverkamp et al. (2005), involves the equivalence of shape parameters. In this conversion approach, the water retention shape index, which is an integral measure of the slope of the retention curve, uses a single

number to describe the retention behavior of a specific soil. For a given soil type, the correspondence of different parameters can be attained by assuming that the shape index is constant for that soil type. Leij et al. (2005) derived the shape indices for both BC and vG and then matched them together to find the correspondence between the shape parameters of BC and VG. In this paper, the study conducted by Leij et al. (2005) was employed to FX's SWR model to find the correspondence of fitting parameters m, n of FX with λ, the fitting parameter in BC. However, integration of FX's retention function is unrealistic and a closed form solution is not available (Gallage et al., 2013).

The above discussed analytical approaches involve evaluation of an integral of each retention function and them matching them together to find any correspondence. The analytical integration of BC's retention function can be evaluated easily and a closed form can be obtained. On the other hand, the analytical integration of the FX's retention function is not possible due to its high non-linearity and a closed form solution cannot be attained. Also, the numerical integration of FX's function is very cumbersome, and it is very difficult to correlate with any other function. Such conduct of FX's function motivated the use of the empirical approach to find the correspondence.

2.4 Methodology

2.4.1 Constrained non-linear optimization

Constrained non-linear optimization method finds a vector that is a local minimum to a scaler function subjected to constraints on the permissible vector. The main objective of constrained optimization is to convert the complex non-linear problem into a simpler equivalent problem that can be solved and used for an iterative procedure. Constrained non-linear optimization to estimate the fitting parameters of the BC and the

FX's function was accomplished using a subroutine "*fmincon*" from Matlab. The fmincon finds a constrained minimum of a multivariate scaler function by improving the fit from an initial guess. To ensure the convergence of the optimized retention data to the measured data, it may be required to define a set of lower and upper bounds for the fitting parameters during the optimization so as to make sure that the solution is always in the range. The multivariate scaler function or the objective function is defined as the root mean square error (RMSE) of the fitted and measured water content values. The fmincon function starts with an initial guess of scaler variable (fitting parameters) within the defined bounds and attempts to minimize the RMSE at that particular guess. The "*fmincon*" function continues to evaluate the RMSE using different scalar variable values within the defined bounds until the RMSE value is minimized. Consequently, the value of the scaler variable at which the lowest RMSE is achieved is the optimized fitting parameter of that function. The optimized fitting parameters are then used in their respective retention functions to generate the corresponding SWRC's. The equation of RMSE for optimization of the retention functions is given as:

$$RMSE = \sqrt{\frac{\sum(\theta_{measured} - \theta_{predicted})^2}{N}} \tag{2.5}$$

where $\theta_{measured}$ is the measured volumetric water content from UNSODA, $\theta_{predicted}$ is the predicted volumetric water content from the respective retention functions (BC or FX) and N is the number of the retention data points.

Therefore, by using the aforementioned method the fitting parameters (θ_s, h_a, λ) for the BC and (θ_s, a, n, m) for the FX were estimated. However, the parameter θ_r which is usually considered as an empirical parameter, is excluded in this study by restraining it

to zero ($\theta_r = 0$). The reason for excluding θ_r is to avoid the likely convergence issues during optimization, as well as the poor predictability and lack of conceptual underpinning (Leij et al., 2002). Also, due to the reason that the FX considers $\theta_r = 0$ (Fredlund and Xing, 1994), therefore, it is considered zero for BC as well. It is recommended that by setting $\theta_r = 0$, retention curves can be fitted more precisely (Phoon et al., 2010). Even though θ_r is considered as a fitting parameter, the results for 601 soil samples from UNSODA showed that almost 50% of the soils have $\theta_r = 0$, and among the rest of the soils, the value for θ_r is close to zero for the majority. To check the accuracy of the results generated from the Matlab subroutine, the fitting parameters acquired for BC were verified by fitting against the SWRC using a non-linear fitting program by Seki (2007).

2.4.2 Developing a parameter conversion equation

The data acquired on various soils were used to develop the parameter conversion between BC and FX. Overall 601 soils were selected from UNSODA. The fitting parameters for each retention function were estimated using the aforementioned method and consequently, SWRC's were evaluated for all the soils by fitting the retention models to the measured data. To convert the parameters of FX to BC, several methods were investigated but due to the difficulty in integrating the FX function, the correlation could not obtained. Consequently, an empirical approach was adopted to find the correspondence between the two functions. The primary phase of parameter conversion is to assess a correlation between the fitting parameters of the models under investigation.

In this study, an empirical equation is proposed to estimate BC parameter (λ) from FX's parameters (m, n) and is given as:

$$\lambda = \frac{m^2 n}{1+3m} \tag{2.6}$$

The proposed equation (2.6) can be used to convert FX's parameters (m, n) to BC parameter and consequently generate the SWRC for BC without fitting the BC model directly to the measured data. An error analysis was performed by evaluating the RMSE between the actual λ and the estimated λ using equation (2.6). The RMSE was calculated by using the following equation:

$$RMSE = \sqrt{\frac{\sum(\lambda_{BCFX} - \lambda_{BC})^2}{N}} \tag{2.7}$$

where λ_{BCFX} is the BC fitting parameter estimated using equation (2.6), λ_{BC} is the optimized BC parameter and N is the number of soils for which the parameters were estimated. RMSE between the parameter λ_{BC} and λ_{BCFX} was calculated for all the 601 soil samples and the comparison is discussed in the following section.

2.5 Results and discussion

2.5.1 Comparison of fitted and estimated λ

The proposed equation (2.6) was tested using statistical analysis (linear regression analysis) by comparing the results obtained from the equation (2.6) with the actual BC's fitting parameter obtained by fitting the model to the measured retention data. Figure 2.3 displays a linear regression through the origin of the BC fitting parameter λ_{BC}, optimized autonomously by fitting to the retention data versus λ_{BCFX} , estimated from FX's fitting parameters using the proposed equation (2.6). The results show a high correspondence and the agreement between λ_{BC} and λ_{BCFX} is strong, with the correlation coefficient $R =$

0.98, coefficient of determination, $R^2 = 0.95$ and the equation of the linear regression as $y = 0.99\ x$ with a slope of almost 1. Moreover, the overall RMSE between λ_{BC} and λ_{BCFX} is 0.097 which shows that the agreement between the two is good. As can be seen from the Figure 2.3, the proposed equation gives realistic values for the estimated parameter, and therefore, can be used to predict the BC fitting parameter λ from FX. To assess the proposed equation further, regression through the orgin for each soil texture is performed. Table 2.1 shows the results of the linear regression analysis and the RMSE between λ_{BC} and λ_{BCFX} for different soil textures.

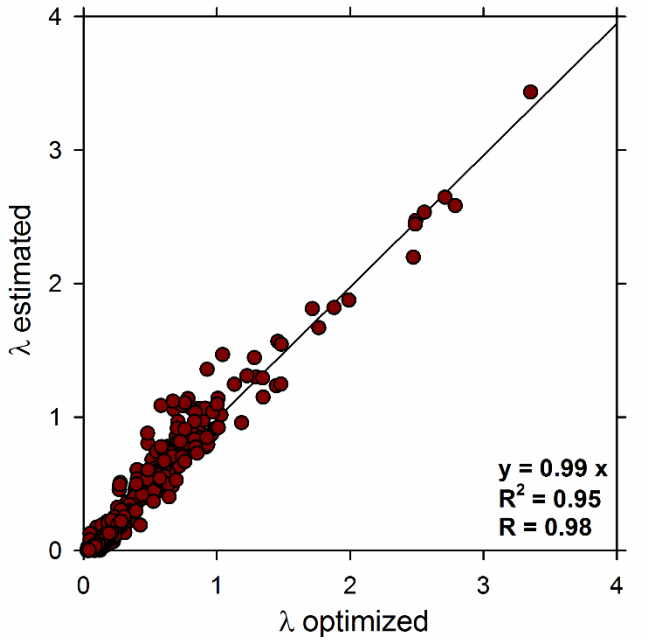

Figure 2.3 Correlation of estimated λ and optimized λ

Fitting parameter λ of BC estimated from FX's parameters using equation (2.6) as a function of optimized λ for 601 samples from UNSODA

Table 2.1 Statistics of regression analysis and the RMSE between λ_{BC} and λ_{BCFX} for different soil textures

Soil Type	Number of soils	RMSE	R2	Correlation Coefficient (R)
Clay Loam	28	0.053	0.903	0.976
Clay	24	0.050	0.273	0.526
Loam	66	0.072	0.729	0.888
Loamy Sand	43	0.063	0.864	0.965
Sand	129	0.142	0.938	0.971
Sandy Clay Loam	47	0.098	0.753	0.908
Sandy Loam	85	0.085	0.904	0.971
Silty Clay Loam	29	0.081	0.795	0.911
Silt Loam	128	0.077	0.836	0.932
Silty Clay	22	0.059	0.667	0.930

The statistics from the Table 2.1 illustrate that the agreement between λ_{BC} and the proposed equation (2.6) is very good for all soil textures with highest R in case of clay loam and lowest in clay. The R^2 values decreased for some soil textures by forcing the regression through the origin. The RMSE for each soil texture is also shown in Table 2.1 with the least value in clay and the highest in sand. Figure 2.4 illustrates the linear regression through the origin for sand and clay. The results in Figure 2.4 (a) show that the correlation between λ_{BC} and λ_{BCFX} for 129 samples of sand is very good with $R = 0.971$, $R^2 = 0.938$ and the equation of linear regression line $y = 1.01\,x$. On the other hand, the

Figure 2.4 (b) shows a poor correlation between λ_{BC} and λ_{BCFX} for 24 samples of clay with $R = 0.526$, $R^2 = 0.273$ and the equation of linear regression line $y = 0.41\,x$. The low correlation for clay is due to the higher difference in λ_{BC} and λ_{BCFX} values for some soil samples. Also, in some cases the value of the parameter h_a of BC is greater than the parameter a of FX.

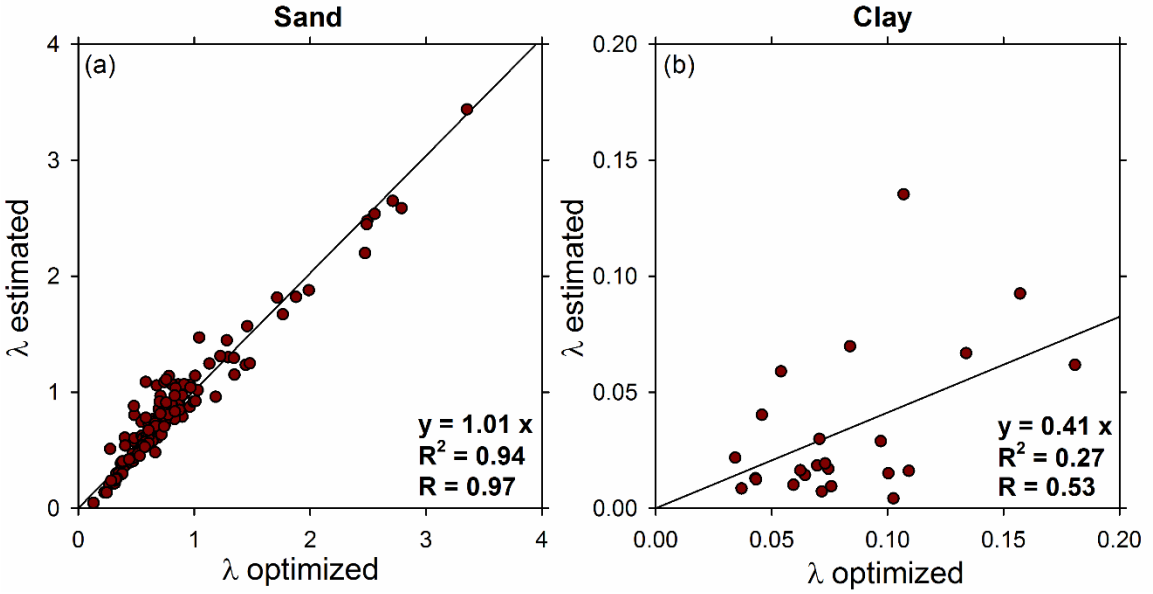

Figure 2.4 Correlation of estimated λ and optimized λ for (a) sand and (b) clay

Relationship between the parameter λ_{BCFX} and optimized λ_{BC} for (a) sand and (b) clay

2.5.2 Comparison of the fitting parameters of BC and FX

The BC's fitting parameters were compared with the corresponding fitting parameter of the FX to investigate any correspondence between them. The comparison was performed based on the linear regression analysis through the origin and the results of the regression analysis are shown in Figures 2.5, 2.6 and 2.7.

Figure 2.5 (a – b) shows the results of the regression analysis for the parameter n of FX as a function of: (a) the BC's parameter λ_{BC} (b) the BC parameter λ_{BCFX} estimated using equation (2.6). As can be seen in the Figure 2.5, the regression analysis through the origin resulted in a poor correlation in both cases. The parameter n controls the slope of the SWRC and its value typically depends on the particle size, with higher values for coarse textured soil resulting in steep curves and lower values in fine textured soils resulting in flat curves (Fredlund et al., 2002). The parameter λ_{BC} is a measure of the slope of the moisture release curve and as such is an indirect measure of the soil's tortuosity. Therefore, coarse textures have higher λ_{BC} values as they have lower tortuosity (Timilin et al., 1999). Although, both the parameters n and λ_{BC} are related to the size of the particles however, the results from Figure 2.5 depict that the relationship between them is poor.

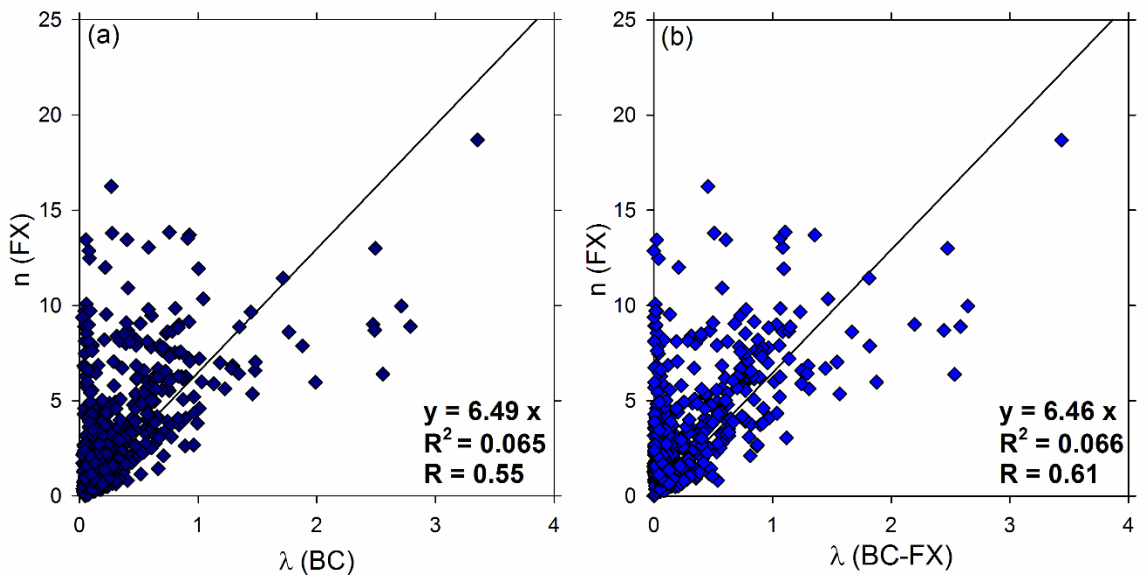

Figure 2.5 Relationship of n with λ_{BC} and λ_{BCFX}

Relationship between the FX's parameter n with the BC's parameter λ_{BC} and the BC parameter λ_{BCFX} estimated from FX's fitting parameters using equation (2.6)

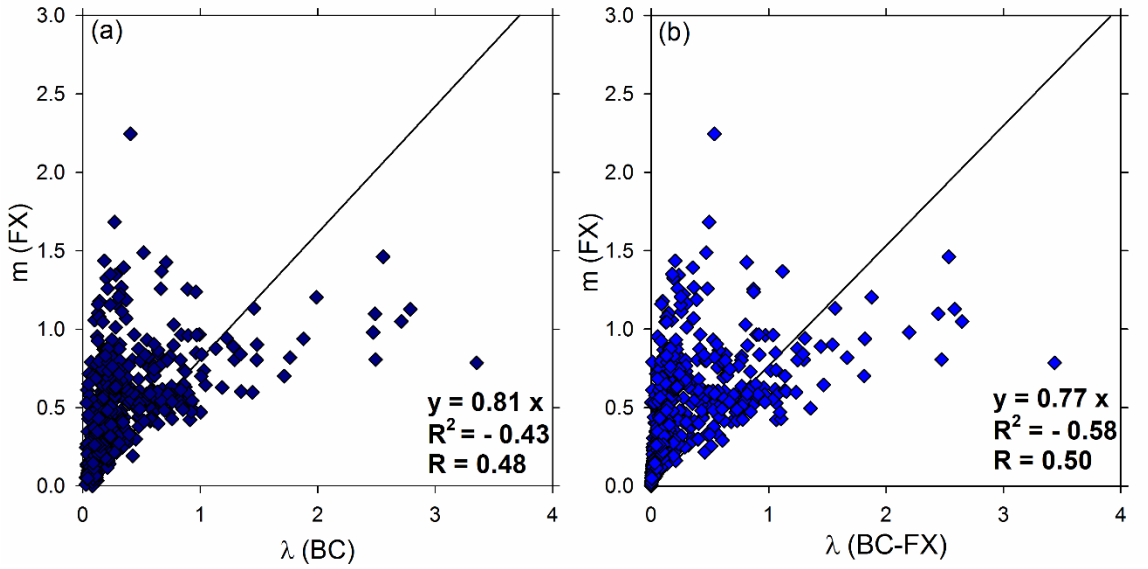

Figure 2.6 Relationship of m with λ_{BC} and λ_{BCFX}

Relationship between the FX's parameter m with the BC parameter λ_{BC} and the BC parameter λ_{BCFX} estimated from FX's fitting parameters using equation (2.6)

The results of the regression analysis through the origin (the no-intercept model), for the parameter m as a function of: (a) λ_{BC} (b) λ_{BCFX} are shown in Figure 2.6 (a – b). The regression results in the negative R^2 which is possible only when the chosen model does not follow the trend of the data, so fits worse than a horizontal line. In this case of regression, the R^2 measures the extent of the variability in the dependent variable about the origin and cannot be related with the models that include an intercept (Eisenhauer, 2003). As can be seen from the Figure 2.6, the correlation between the parameter m and (a) λ_{BC} (b) λ_{BCFX} is very poor with R of 0.48 and 0.5 respectively.

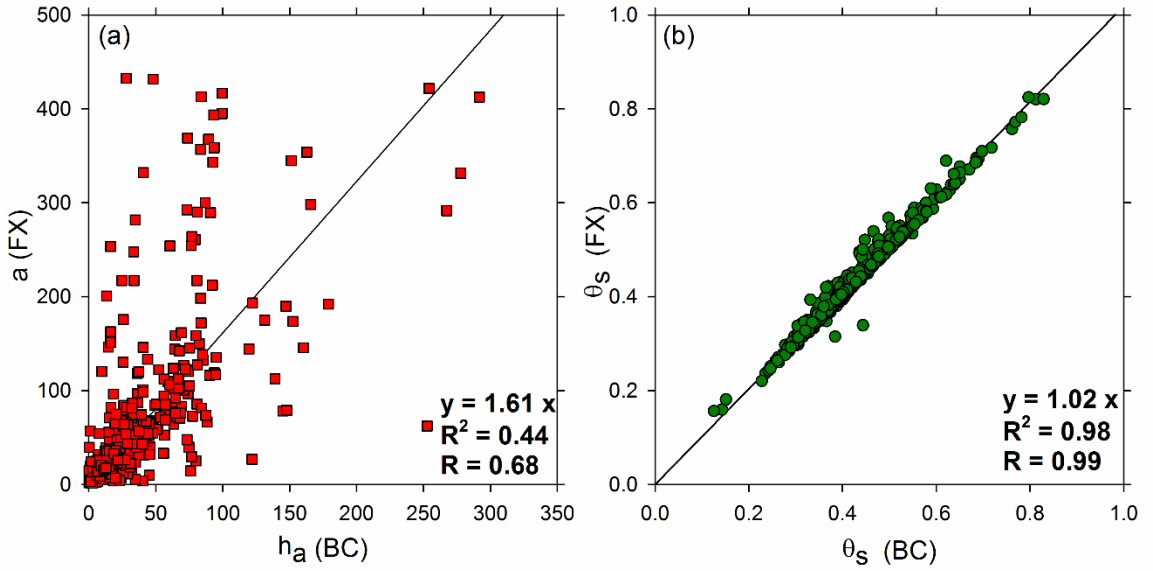

Figure 2.7 (a) Correlation between a (FX) and h_a (BC) (b) Correlation between θ_s obtained from FX and BC's retention functions

(a) Correlation between the parameter a obtained from FX's retention function and the parameter h_a obtained from BC's retention function for 601 soils from UNSODA. (b) Correlation between the parameter θ_s obtained from FX and BC's retention functions for 601 soils from UNSODA

Figure 2.7 (a) shows a relationship between the corresponding fitting parameters of FX and BC's retention functions. The fitting parameter h_a in BC has been shown to be approximately related to the parameter a in the FX with $R = 0.68$, $R^2 = 0.44$ and the equation of the linear regression line is given by $y = 1.61\ x$ with a slope of 1.61. The parameter $a\ (FX)$ is usually higher than the parameter $h_a(BC)$, specifically when the other fitting parameters (m, n) of FX's retention model tend to reach towards their extreme values. However, for smaller values of the parameter $m\ (FX)$, the parameter a can be considered equal to the parameter h_a (Fredlund and Xing, 1994) and from Figure 2.7 (a) it can be seen that the parameter a is in satisfactory agreement with the parameter h_a. Whereas, Figure 2.7 (b) shows a relationship between the parameter $\theta_s\ (FX)$ and $\theta_s\ (BC)$, with $R = 0.68$, $R^2 = 0.98$ and the slope of 1.02 for the linear regression line. The results in Figure 2.7 (b) illustrate that the parameters $\theta_s\ (FX)$ and $\theta_s\ (BC)$ are in good agreement with each other and can be therefore linearly correlated to each other.

2.5.3 Predicted retention curves of BC, FX, and BC using FX

The measured retention data for 601 soil samples with different textures is shown in Tables 2.2 and 2.3 for BC and FX's retention functions respectively. Each table is presented with the number of soils from particular texture, including the fitting parameters of each retention model. The fitting parameters were obtained by non-linear constrained optimization within the defined limits. For each fitting parameter, there is shown a calculated minimum, maximum, mean and standard deviation.

Table 2.2 Fitted Brooks & Corey model parameters and soil properties of the 601 soil samples from UNSODA. '#' represents the number of soils

Soil Type	#	θ_s				h_a				λ			
		Min	*Max*	*Mean*	*S.D*	*Min*	*Max*	*Mean*	*S.D*	*Min*	*Max*	*Mean*	*S.D*
Clay Loam	28	0.34	0.76	0.47	0.10	0.12	63.29	18.42	16.72	0.03	0.61	0.12	0.11
Clay	24	0.37	0.72	0.51	0.08	0.20	252.63	39.70	57.12	0.03	0.18	0.08	0.04
Loam	66	0.31	0.83	0.47	0.11	1.76	147.75	26.75	27.23	0.04	0.63	0.15	0.09
Loamy Sand	43	0.26	0.55	0.38	0.06	2.40	62.12	17.93	10.70	0.09	0.93	0.40	0.16
Sand	129	0.13	0.48	0.35	0.06	3.60	94.66	21.47	14.98	0.13	3.35	0.83	0.57
Sandy Clay Loam	47	0.30	0.60	0.40	0.06	0.76	119.67	27.29	28.64	0.04	0.69	0.15	0.15
Sandy Loam	85	0.24	0.54	0.38	0.07	1.50	165.50	32.42	31.69	0.04	1.48	0.27	0.23
Silty Clay Loam	29	0.23	0.80	0.52	0.12	6.12	179.04	37.13	39.36	0.03	0.43	0.14	0.08
Silt Loam	128	0.31	0.78	0.43	0.07	0.15	291.73	51.74	50.34	0.02	0.92	0.19	0.14
Silty Clay	22	0.32	0.70	0.54	0.09	6.72	160.20	29.61	35.49	0.04	0.19	0.10	0.04

Table 2.3 Fitted Fredlund & Xing model parameters and soil properties of the 601 soil samples from UNSODA. '#' represents the number of soils

Soil Type	#	θ_s				a				n				m			
		Min	*Max*	*Mean*	*S.D*	*Min*	*Max*	*Mean*	*S.D*	*Min*	*Max*	*Mean*	*S.D*	*Min*	*Max*	*Mean*	*S.D*
Clay Loam	28	0.34	0.76	0.47	0.10	1.98	120.08	33.00	28.87	0.07	8.14	2.40	2.06	0.03	0.61	0.25	0.16
Clay	24	0.37	0.72	0.52	0.09	2.24	118.61	26.66	28.67	0.41	8.91	2.86	2.51	0.04	0.60	0.17	0.13
Loam	66	0.31	0.82	0.48	0.11	1.55	200.75	45.04	52.93	0.23	10.07	2.12	1.82	0.04	1.06	0.34	0.25
Loamy Sand	43	0.26	0.53	0.38	0.06	2.01	104.09	30.80	17.30	0.87	13.71	4.06	2.61	0.10	1.39	0.57	0.26
Sand	129	0.16	0.48	0.35	0.05	5.07	158.77	32.24	23.90	0.83	18.70	5.86	3.30	0.14	2.25	0.72	0.29
Sandy Clay Loam	47	0.31	0.63	0.40	0.06	1.98	146.08	40.85	39.76	0.01	8.99	2.61	2.36	0.03	1.37	0.32	0.27
Sandy Loam	85	0.24	0.55	0.38	0.07	3.85	432.59	65.10	83.31	0.36	16.25	3.14	3.02	0.03	1.35	0.45	0.24
Silty Clay Loam	29	0.22	0.82	0.53	0.12	5.73	191.97	51.34	45.05	0.70	12.48	2.83	2.33	0.03	0.60	0.22	0.15
Silt Loam	128	0.31	0.78	0.44	0.07	1.10	431.39	119.33	117.70	0.24	13.46	1.70	2.07	0.00	1.68	0.52	0.35
Silty Clay	22	0.33	0.71	0.55	0.09	13.91	145.47	37.58	35.42	0.66	9.72	3.47	2.37	0.03	0.83	0.18	0.17

The results from Tables 2.2 and 2.3 show that for fine textured soils (e.g., loam, silty clay loam, clay), the value for θ_s tends to revert to their maximum values whereas the coarse textured soils (e.g., sand, sandy loam) have lower values. From Table 2.2, the results show that the parameter λ which is related to the pore size, has higher values for coarse soil textures with the highest value in case of sand, while, the clay has the least value. From Table 2.3, similar behavior can be observed in case of the parameters $m(FX)$ and $n(FX)$ with highest value in sand and the least values for m in clay and for n in clay loam. The results for the parameter h_a from Table 2.2 show that the silty loam and the clay soil textures have highest values and the least values are seen in the loamy sand and the clay loam. From Table 2.3, for the parameter a, the silt loam and sandy loam have uppermost values and the loamy sand has the smallest value. The results of the parameter C_r that represents the soil suction at the residual water content are not included in Table 2.2, because this parameter is usually assumed to be constant. Although, the parameter C_r was evaluated during the optimization between the bounds (20 – 9000). The value of C_r for most of the soils was in the range of 2000 – 4000 and for some soils its value reached the defined upper bound (9000) which means that in these soils the value of C_r tends to infinity. The upper bound for the parameter C_r was kept at 9000 because the curve was not sensitive to the higher values.

Figure 2.8 (a – j) illustrates the fitting of the measured retention data (lab drying) from the UNSODA corresponding to the two SWR functions given by BC and FX for 10 soil textures on a semi-log plot. Each subfigure (a – j), represents a particular soil texture and the soil selected from each texture is represented by an identification code used in UNSODA. Moreover, a third SWRC is generated using the BC function, but the fitting

parameters are estimated from the FX function as:$\theta_s(BC) = \theta_s(FX)$, $\lambda = \frac{mn}{1+3m}$, and $h_a = a$. The assumption that $h_a = a$ is valid for only smaller m values, because the parameter a usually has higher value than the air entry value (Fredlund and Xing, 1994). This may cause some discrepancies in the fitting of the curve and may result in over estimation of the air entry value (h_a). The results in Figure 2.8 suggests that the predicted BC retention curve from FX (BC-FX) is similar to the actual BC retention curve for all soil textures. As can be seen from Figure 2.8, the fine textured soils (e.g., clay) have flat curves whereas the coarse textured soils (e.g., sand) have sharp curves. The aforementioned results and discussion show that the proposed method can be used to predict BC fitting parameters and generate the corresponding retention curve. But, the conversion cannot work the other way i.e., the FX parameters (m, n) cannot be predicted from the BC parameter (λ), unless some assumptions are made or some relation is developed between m and n. The reason for this is that two parameters cannot be derived from a single parameter. Therefore, additional equivalence between the parameter m and the parameter n should be developed to reduce the number of fitting parameters and the conversion from BC to FX.

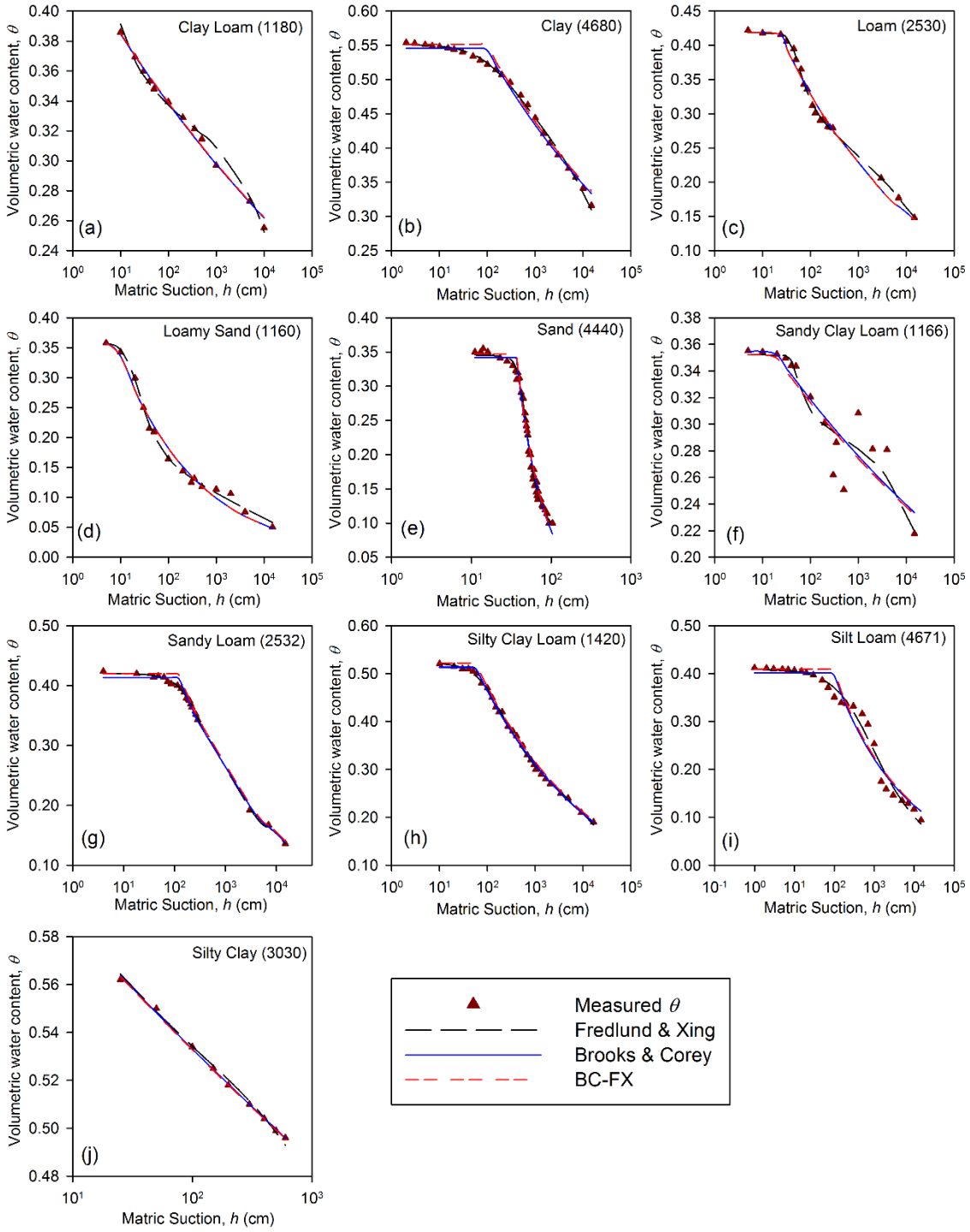

Figure 2.8 Comparison of fitted BC, FX and BC-FX with the measured data

Comparison of fitted Brooks & Corey (BC), Fredlund and Xing (FX) and the estimated Brooks and Corey using Fredlund and Xing (BC-FX) with the measured data for 10 soil textures

CHAPTER III

COUPLED AND UNCOUPLED EARTH PRESSURE PROFILES IN UNSATURATED SOILS UNDER TRANSIENT FLOW

3.1 Introduction

In the context of classical soil mechanics, the lateral earth pressure was estimated using Terzaghi's effective stress. The soil above the water table is unsaturated due to transpiration and evaporation (Fredlund and Rahardjo 1993, Lu and Godt 2013). Despite the fact that the pore water pressure in the vadose zone is negative, the pore water pressure is assumed as zero above the water table in Terzaghi's approach. In unsaturated soil mechanics, the negative pore water pressure in the vadose zone is a function of precipitation intensity, duration and deformation interaction (Wu et al 2011; Wu et al 2013; Wu et al 2015; Wu et al 2016). This dynamic process may increase or decrease the lateral earth pressure (active/passive) which might contribute to various infrastructural problems such as failure or at least the poor performance of the retaining walls, basement walls, pile foundations, tunnels, and sewers.

The increased lateral earth pressure typically reduces the factor of safety against overturning and sliding failure for retaining walls. The increased lateral earth pressure contributes to the development of cracks in basement walls, tunnels and sewers and most likely, resulting in the collapse of these structures. Damages caused due to the changes in lateral earth pressure in the USA reached to 13$ billion (Puppala and Cerato, 2009) from

2.3$ billion (Jones and Holtz, 1973) in the last four decades. The necessity of considering these parameters in the service state of existing geo-structures warrants the government agencies, contractors, owners, consultants and insurance companies to invest significant attention and financial resources to deal with this problem (Day 1994).

The instability of retaining structures in unsaturated soils due to precipitation incidence (Yoo and Jung 2006; Kim and Borden 2013; Koerner and Koerner 2013; Valentine 2013; Zhang et al. 2010) emphasizes that the vadose zone should be considered as an unsaturated region above the water table including two subzones: seasonally unsteady and steady zone. Figure 3.1 shows the different zones in an unsaturated soil. The time-dependent zone is at the top, which is influenced by environmental factors i.e., precipitation, evaporation, and airflow conditions. This zone is called as unsteady or active zone. In this zone soil suction is dependent on time, while below the active zone the zone is called as steady zone where the soil suction is independent of time and governed by hydrological and geological conditions (soil type), recharge rate, and surface topography (Lu and Likos 2004).

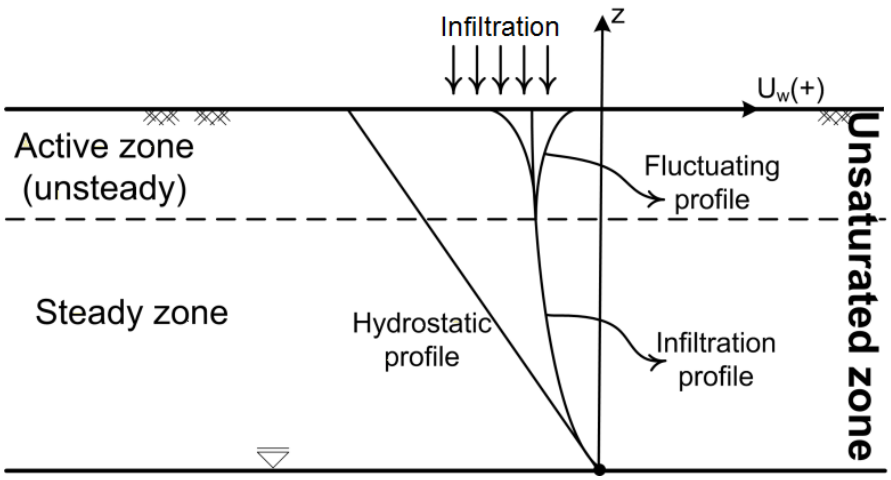

Figure 3.1 Active and steady zone in unsaturated soil under transient flow

In the last few decades, several numerical, analytical, and experimental studies have been performed to study the influence of matric suction on the earth pressure for unsaturated retaining structures (Fredlund and Rahardjo 1993; Blake et al 2003; Lu and Likos 2004; Vo and Russell 2014; Vahedifard et al 2015; Vo and Russell 2016). Due to the complexity of matrix suction simulation in the analytical methods and its variable characteristic in different soil types, the numerical methods for unsaturated soils are commonly used. To find the lateral earth pressure in unsaturated soil, employing simplified assumptions are common in practice. For example, solving the one-dimensional flow, a hydrostatic variation of matric suction in the unsaturated zone, or using a constant rate of change in shear stress as a function of matric suction are the well-known assumptions (Fredlund and Rahardjo 1993; Lu and Likos 2004; Tavakoli and Vanapali 2011).

In general, the term suction stress is more practical to represent the state of stress in the analysis of lateral earth pressure since matric suction is an independent stress

variable (Lu 2008). Fredlund and Morgenstern (1977) introduced an independent stress state variable to evaluate the shear strength. Later, it was proved that the matric suction angle, ϕ^b which represents the effect of matric suction, is not constant (Vanapalli et al 1996). Moreover, shear strength depends on increase or decrease in matric suction which leads to increase or decrease in shear strength of soil, respectively. The changes in matric suction repeatedly occur in vadose zone. For example, the increase in rain intensity or rate of infiltration leads to increase in water content and decrease in matric suction whereas evaporation increases the matric suction and decreases the water content. In addition, the profiles of matric suction diverge from the hydrostatic conditions under different steady state flow rates (Lu and Likos 2004, 2006).

Vanapalli and Fredlund (2000) showed that the shear strength is indirectly influenced by the soil water characteristic curve (SWCC) and introduced the parameter suction stress as a function of the effective degree of saturation based on experimental results from unsaturated shear strength tests. The resulting suction stress contributes to extend the Bishop's (1959) effective stress principle to be used in Mohr-Coulomb failure envelope for estimating the shear strength of unsaturated soils. However, Bishop's effective stress approach does not consider the physicochemical interaction in silty and clayey soils, and therefore, resulting in nonzero suction stress. In addition, the effective stress is not a monotonic function of matric suction and subsequently, the Bishop's effective stress hardly leads to accurate results for higher matric suction (Vahedifard et al 2015). Lu and Likos (2004, 2006) used the effective stress parameter for characterizing the suction stress as a function of matric suction. Based on this approach, the suction

stress is not a constant and varies nonlinearly in vadose zone in which the non-monotonic nature of effective stress variation is preserved.

In the above-mentioned literature, the effect of deformation on pore water pressure calculation has not been considered. Recently, the mechanical behavior of the unsaturated soils due to changes in negative pore water pressure during the infiltration is the subject of several studies (e.g. Wang and Li 2005; Wu and Zhang 2009; Zhan et al 2013; Zhao and Zhang 2014; Wu et al 2015; Wu et al 2016). Several analytical coupled models of infiltration proposed by Wu et al., suggesting that coupling of infiltration and deformation is very important for the study of infiltration in unsaturated soils. Also, the initial condition plays a crucial part in the coupling effect and re-distribution of the pore water pressure.

The effect of hydraulic behavior (i.e., suction) on the mechanical behavior leads to increase in pre-consolidation pressure and shear strength. However, the compressibility decreases. On the other hand, the effect of the mechanical behavior on the hydraulic behavior leads to shifting of the SWRC which allows one to measure the vertical distribution of matric suction. This shows that the coupling of infiltration and deformation are very crucial in the study of unsaturated soils. The coupling effect is more profound in the soils which undergo a considerable deformation as a result of the infiltration. However, for well-compacted engineered coarse grained soils where deformation is not considerable, the effect of coupling reduces and does not have a noticeable contribution to variation of stress profiles. Moreover, the uncoupled analysis is much easier and does not include the role of deformation. The stress changes also affect the flow rate and the negative pore water pressure profile in the soil body (Cho and Lee

2001; Zhang et al. 2011). This statement implies the importance of coupled formulation of infiltration and stress-deformation in lateral earth pressure calculation.

In this study, we present a numerical framework to determine the matric suction from coupled/uncoupled unsaturated infiltration and deformation due to the rainfall. In order to formulate the coupled approach, the constitutive equation for the SWRC is defined based on the Gardner's equation (1985). The equations that govern the coupled infiltration and the deformation in an unsaturated soil are obtained using Darcy's flow law, continuity equation, and fluid mass conservation law, and Richard's equation which is linearized by the exponential hydraulic conductivity and moisture content relationships. Subsequently, the derived matric suction in various time intervals is assembled to suction stress-based effective stress relationship (Lu and Likos 2006). The use of suction stress-based effective stress allows prediction of lateral earth pressure even in high suction values (i.e., when saturation is low). The shear strength parameters ϕ' and c'also included as components in unified effective stress that leads to a simple shear strength calculation without introducing additional parameters. Subsequently, the associated components are used in Rankin's state of failure criterion to demonstrate the variation of active and passive earth pressure in different soil types and time scenarios.

3.2 Previous studies on lateral earth pressure in unsaturated soils

Estimation of the lateral earth pressures (active/passive) imposed by the soils on the retaining structures is very important. Especially, when changes in volumetric water content and matric suction in the unsaturated soils considerably change the lateral earth pressure (Yelti et al 2011). On the other hand, the unsaturated soils behind the retaining structures lead to conservative designs (Tavakkoli and Vanapalli 2011). Pufhal et al

(1982) and Hong (2008) related the variations in the degree of saturation in the backfill soils to the increase in lateral earth pressure in expansive soils. Fredlund and Rahardjo (1993) introduced the active and passive unsaturated earth pressures based on Rankin's theory. Zhang et al (2010) used Rankin's state of failure to introduce active earth pressure in unsaturated soils while Liang et al (2012) obtained a solution for the active earth pressure based on Coulomb's earth pressure parameters and changes in matric suction. Vahedifard et al (2015) presented a framework for estimating the lateral earth pressure under steady flow in unsaturated soils based on log-spiral mechanism. They used suction stress based effective stress as a component in the limit equilibrium, which resulted in reasonable approach in defining the lateral earth pressure in unsaturated soils.

The aforementioned studies attempted to determine the lateral earth pressure due to changes in matric suction in the steady zone of unsaturated soils. In addition, they did not consider the effect of changes in stress state, which closely defines the mechanical deformation of the soil body. The point of interest of this study is the evaluation of passive and active earth pressure profiles in the active zone where the matric suction is a function of time and depth. Moreover, the negative pore water pressure is obtained from numerical solution of coupled infiltration and deformation due to rainfall. Coupled unsaturated infiltration and stress-deformation formulation is derived from the equilibrium of the soil structure and unsaturated fluid flow in porous media (Lioret et al. 1987; Alonso et al. 1989; Thomas and He 1995; Kim 2000; Ravichandran 2009). The first coupled constitutive formulation can be called as flow and deformation analysis of partially saturated soil by Lioret et al. (1987). Thomas and He (1995) introduced the thermo-hydro-mechanical model in unsaturated medium and solved the coupled

governing equations using the finite element method. The unsaturated hydro-mechanical model is also used in the simulation of coupled water-table fluctuation and land deformation under prescribed loading (Kim 2000). However, this paper, in a numerical framework, proposes a variable lateral earth pressure formulation by considering the coupling effect of infiltration and deformation. In addition the effect of residual water content is considered in the present work.

3.3 Theory

Some presumptions required to arrive at the governing equations for one dimensional coupled hydro-mechanical model include:

- The porous medium liquid should obey Darcy's Law.
- The compressible behavior of pore water is ignored, whereas the deformable behavior of the soil structure is considered.
- The variation in volume is considered as a result of changes in effective stress and not as a result of the variations in total stress.
- The pore air pressure is considered constant throughout the soil domain.

3.3.1 Effective stress in partially saturated soils

The unified effective stress approach is the most influential method for evaluating the behavior of the saturated and the unsaturated soils. This approach changes the problem from a multi stress, multiphase permeable medium to a single-stress continuous medium, permitting the major applications of solely solid mechanics to the deformable permeable media containing liquid. Unified effective stress, which is the extension of the Bishop's effective stress (1959), considers the inter-particle forces interaction. This consideration leads to a realistic representation of non-zero suction for fine materials i.e,

clay and silt (Vahedifard and Rabinson 2015). Further discussion along with experimental verifications to determine the role of inter-particle forces including Van der Waals forces, electrical double layer forces, forces from negative pore-water pressure, and et al., can be found in Lu and Likos (2006). The unified effective stress for saturated and unsaturated conditions is defined as:

$$\sigma' = (\sigma - u_a) - \sigma^s \tag{3.1}$$

where σ' is the effective stress, σ^s represents the suction stress, and u_a represents the atmospheric pressure which is considered ($u_a = 0$) in this study (Lu and Likos 2006). Lu et al. (2010) introduced σ^s as a function of effective degree of saturation:

$$\sigma^s = \begin{cases} -(u_a - u_w) & (u_a - u_w) < 0 \quad (a) \\ -S_e(u_a - u_w) & (u_a - u_w) \geq 0 \quad (b) \end{cases} \tag{3.2}$$

$$S_e = \frac{\theta - \theta_r}{\theta_s - \theta_r} \qquad (c)$$

In the above equations, u_w is the negative pore pressure, S_e represents the effective degree of saturation, θ_r is residual volumetric moisture content, and θ_s represents the saturated volumetric moisture content and θ represents the volumetric water content. Eq. (3.1) simply represents Terzaghi's effective stress by replacing Eq. (3.2a) into Eq. (3.1). Moreover, Eq. (3.2c) shows that the effect of relative saturation allows predicting suction stress even in dry soils (Lu et al 2010).

Gardner (1985) introduced a nonlinear function in exponential form to represent the Hydraulic Conductivity Function (HCF) and SWRC. This model relies only on one fitting parameter (α) and is widely used in literature (Lu and Likos 2004; Yeh 1989; Srivastava and Yeh 1991, Lu and Godt 2013). The reciprocal of the vertical height of the capillary fringe (α) shows that the increase in the negative pore pressure decreases θ, S_e,

and hydraulic conductivity. In addition, the parameter α has a major impact on the pressure head profiles, as during the initial infiltration there is greater reduction of the matrix soil suction for larger values of α. HCF function based on Gardner's representation follows:

$$k = k_s e^{-\alpha(u_a - u_w)} \tag{3.3}$$

where k is relative permeability and k_s is the hydraulic conductivity in fully saturated condition. The extension of Gardner's definition for SWRC represents the dependency of degree of saturation to matric suction as:

$$\theta = \theta_r + (\theta_s - \theta_r)e^{-\alpha(u_a - u_w)} = \theta_r + (\theta_s - \theta_r)S_e \tag{3.4}$$

This closed-form equation for the suction stress profile is followed by the assumption that can be used to obtain the coupled formulation for considering transient seepage and deformation.

Based on the assumption that the volume change of the soil is due to the change in the effective stress only, the total stress change is not considered, and u_a is assumed as 0. Therefore, using Eq. (3.1) and taking its partial derivative with respect to time, we have

$$\frac{\partial \sigma'}{\partial t} = \frac{\partial}{\partial t}\left((\sigma - u_a) - \sigma^s\right) = -\frac{\partial}{\partial t}(S_e u_w) \tag{3.5}$$

Using Isotropic Hook's law and substituting the effective stress tensor (σ'_{ij}) in the constitutive relation of the soil structure gives:

$$\varepsilon_{ij} = \frac{-\lambda\delta_{ij}}{2G(3\lambda+2G)}\sigma'_{kk} + \frac{1}{2G}\sigma'_{ij} \tag{3.6}$$

where λ and G are the two independent Lame's elastic constants, and δ_{ij} is Kronecker delta. According to linear elastic theory the two independent Lame's elastic constants can

be expressed as functions of Young's modulus (E) and the Poisson's ratio (ν) (i.e., strain in a particular direction) as:

$$\lambda = \frac{\nu E}{(1+\nu)(1-2\nu)}; G = \frac{E}{2(1+\nu)} \tag{3.7}$$

Solving Eq. (3.6) by substituting the two Lame's constants, we obtain

$$\varepsilon_{ij} = -\frac{\nu}{E}\delta_{ij}\sigma'_{kk} + \frac{(1+\nu)}{E}\sigma'_{ij} \tag{3.8}$$

where for or a 1D problem, the strain in other two directions are zero i.e., $\varepsilon_{xx} = \varepsilon_{yy} = 0$, therefore, we have

$$\varepsilon_{zz} = \frac{(1-\nu-2\nu^2)}{E(1-\nu)}\sigma'_{zz} \tag{3.9}$$

where $\varepsilon_{zz} = \frac{\partial u}{\partial z}$; ε_{zz}, u and σ'_{zz} represent the strain, displacement and effective stress in the z- direction respectively.

Taking the partial derivative of Eq. (3.9) with respect to time on both sides and replacing the strain in z direction (ε_{zz}) with the volumetric strain ($\varepsilon_v = \varepsilon_{xx} + \varepsilon_{yy} + \varepsilon_{zz}$).

$$\frac{\partial \varepsilon_v}{\partial t} = \frac{1}{B}\frac{\partial \sigma'_{zz}}{\partial t} \tag{3.10}$$

where $B = \frac{E(1-\nu)}{(1-\nu-2\nu^2)}$

The above equation can be written in terms of suction head by using the Eq. (3.1) and the relation $\psi = \frac{u_w}{\gamma_w}$,

$$\frac{\partial \varepsilon_v}{\partial t} = -\frac{\gamma_w}{B}\frac{\partial}{\partial t}(S_e\psi) \tag{3.11}$$

where γ_w is the unit weight of water.

Solving the Eq. (3.11), we have the relation for the rate of change in the volumetric strain as:

$$\frac{\partial \varepsilon_v}{\partial t} = -\frac{\gamma_w}{B}\left(S_e + \psi \frac{\partial S_e}{\partial \psi}\right)\frac{\partial \psi}{\partial t} \tag{3.12}$$

3.3.2 Coupled and uncoupled governing equations for one dimensional infiltration

For isothermal conditions, Darcy's law describes the flow in unsaturated soil as the specific velocity of discharge of a liquid through a porous medium (soil) due to the difference in suction is directly proportional to the matric suction gradient in the direction of flow and is given as:

$$q = -K(\psi)\frac{\partial h_t}{\partial z} \tag{3.13}$$

where q is the specific discharge, h_t is the total soil water head potential. The total soil water head can be considered using only the suction head and the gravitational head as $h_t = h_m + h_g = \psi + z$; where h_m is the matrix suction (ψ) and h_g is the gravitational head or elevation head (z). Therefore, Eq. (3.13) becomes:

$$q = -K(\psi)\frac{\partial}{\partial z}(\psi + z) \tag{3.14}$$

According to the conservation of mass, for a representative elementary volume of soil with porosity *n,* volumetric moisture content *θ,* and density of water *ρ*.

Total flow rate = Rate of inflow – Rate of outflow = Change in Mass Storage

$$-\frac{\partial(\rho q)}{\partial z} = \frac{\partial(\rho\theta)}{\partial t} \tag{3.15}$$

However, we know degree of saturation $S_e = \frac{\theta}{n}$. Therefore, the above equation becomes:

$$-\frac{\partial}{\partial z}(\rho q) = \theta\frac{\partial \rho}{\partial t} + \rho.n.\frac{\partial S_e}{\partial t} + \rho.S_e\frac{\partial n}{\partial t} \tag{3.16}$$

But the derivative of porosity with respect to time (Wu et al., 2009) can be expressed as:

$$\frac{\partial n}{\partial t} = (1-n)^2.\frac{\partial e}{\partial t} = -\frac{(1-n)^2}{1-n_0}\frac{\partial \varepsilon_v}{\partial t} = -\eta\frac{\partial \varepsilon_v}{\partial t} \tag{3.17}$$

where e is the void ratio, ε_v is the volumetric strain and n_0 is the initial porosity of the soil and η is defined as the porosity index. The porosity index is defined as a function of initial porosity and actual porosity of the soil and can be related as:

$$\eta = \frac{(1-n)^2}{1-n_0} = \frac{(S_e-\theta)^2}{S_e^2(1-n_0)} \tag{3.18}$$

The flow in unsaturated soils can be characterized by the Richard's equation which defines the matric suction head and the hydraulic conductivity as the highly non-linear functions of soil volumetric water content. Therefore, relating Eq. (3.14) with Eq. (3.16), Eq. (3.17) and Eq. (3.18), we have the one-dimensional coupled hydro-mechanical governing equation for unsaturated soils as:

$$\frac{\partial}{\partial z}\left(K(\psi)\frac{\partial}{\partial z}(\psi+z)\right) = \frac{\theta}{\rho}.\frac{\partial \rho}{\partial \psi}\frac{\partial \psi}{\partial t} + n.\frac{\partial S_e}{\partial \psi}\frac{\partial \psi}{\partial t} - S_e.\eta\frac{\partial \varepsilon_v}{\partial t} \tag{3.19}$$

Assuming the pore water to be incompressible, and substituting Eq. (3.12) in the above equation gives us the equation of the coupled infiltration and deformation of one-Dimensional problem in unsaturated soils as:

$$\frac{\partial}{\partial z}\left(K(\psi)\frac{\partial}{\partial z}(\psi+z)\right) = n.\frac{\partial S_e}{\partial \psi}\frac{\partial \psi}{\partial t} + S_e.\eta\left(\frac{\gamma_w}{B}\left(S_e + \psi\frac{\partial S_e}{\partial \psi}\right)\frac{\partial \psi}{\partial t}\right) \tag{3.20}$$

The above equation can also be represented as:

$$\frac{\partial}{\partial z}\left(K(\psi)\frac{\partial}{\partial z}(\psi+z)\right) = \left\{\frac{\theta(\psi)}{S_e}.\frac{\partial S_e}{\partial \psi} + \frac{\gamma_w S_e \eta}{B}\left(S_e + \psi\frac{\partial S_e}{\partial \psi}\right)\right\}\frac{\partial \psi}{\partial t} \tag{3.21}$$

This formulation couples the unsaturated seepage and soil skeleton deformation to obtain matric suction. The results can be considered along with Eq. (3.1) to extend the Rankin's theory.

The uncoupled governing equation (Richards' equation) for the infiltration can be obtained by ignoring the deformation of the unsaturated soil as:

$$\frac{\partial}{\partial z}\left(K(\psi)\frac{\partial}{\partial z}(\psi+z)\right)=\frac{\partial\theta(\psi)}{\partial\psi}\frac{\partial\psi}{\partial t} \tag{3.22}$$

To compare the effect of coupling and uncoupling in finding lateral earth pressure Eq. (3.21) and Eq. (3.22) are used to define coupled and uncoupled scenarios.

3.3.3 Extended Rankine's theory for lateral earth pressure

3.3.3.1 Active earth pressure

Rankine's state of failure demonstrates that in the active mode, the failure occurs from the stress which is generated from soil-weight rather than external loads. Rankin uses several unique features to simply express the failure or limit state analysis. The frictionless boundary allows the lateral movement of the soil mass and also the reduction in horizontal stress. Moreover, this assumption allows us to define principal stresses along the vertical and horizontal directions whereby the maximum and minimum principal stresses are acting vertically and horizontally respectively. Implementation of the Mohr-Coulomb criterion in active mode allows one to introduce the state of stress at failure as (Lu and Likos 2004):

$$\sigma_h' = \sigma_v' K_a - 2c'\sqrt{K_a} \tag{3.23}$$

where σ_h' represents the horizontal effective stress, σ_v' represents the vertical effective stress, and K_a is the coefficient of Rankine's active earth pressure which is defined as:

$$K_a = \tan^2\left(\frac{\pi}{4}-\frac{\phi'}{2}\right) \tag{3.24}$$

In the presence of suction stress in unsaturated soil, one can extend the Eq. (3.23) by the incorporation of Eq. (3.1). The extended Rankine's active stress in unsaturated zone is defined as:

$$(\sigma_h - u_a) = (\sigma_v - u_a)K_a - 2c'\sqrt{K_a} - (K_a - 1)\sigma^s \tag{3.25}$$

In the above equation the first two terms on the right hand side represent the original Rankine's theory but the third term shows the extension of classical Rankine's theory compounded with suction stress. In a homogenous soil, it is evident that the first term contributes to the compressive earth pressure in the soil body or the adjacent retaining structures while the second and third term contribute to the tensional stresses due to nature of suction stress. Figure 3.2 shows the contribution of each component in Eq. (3.25) to generate lateral earth pressure.

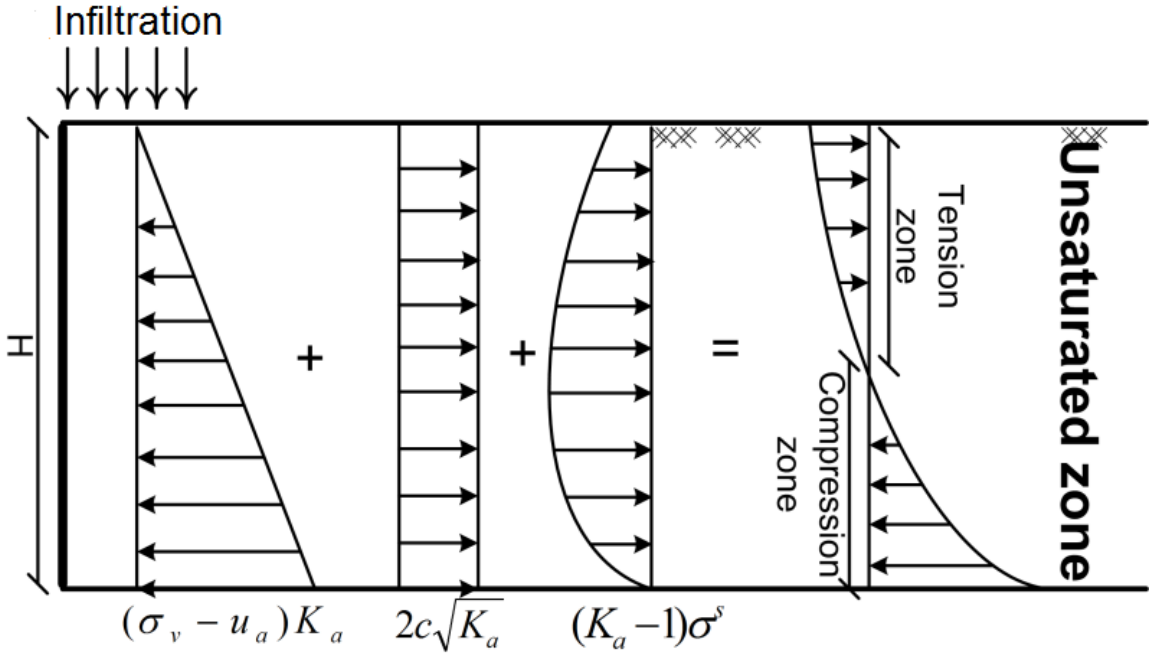

Figure 3.2 Tension and compression stresses under transient flow in active mode of failure

In the absence of surcharge, the contribution of soil weight in the lateral earth pressure increases linearly with depth. The second term which reflects the contribution of mobilized cohesion at the failure state is a constant value in depth. However, the third

component nonlinearly changes with depth and time. According to Eq. (3.25), the coefficient of active earth pressure for unsaturated soil K_{au} can be defined as:

$$K_{au} = \frac{\sigma_h - u_a}{\sigma_v - u_a} = K_a - \frac{2c'\sqrt{K_a}}{\sigma_v - u_a} - \frac{(K_a - 1)\sigma^s}{\sigma_v - u_a} \tag{3.26}$$

The role of suction stress component in K_{au} is highlighted when tensional stress appears in the soil body and causes soil to crack. In the tensional cracked zone the lateral earth pressure is null and earth pressure profile moves from tension zone to the compression zone. In this condition K_{au} is zero and the depth of tension crack (D_t) can be calculated as:

$$D_t = \frac{2c\prime}{\gamma\sqrt{K_a}} + \frac{\sigma^s}{\gamma}\left(1 - \frac{1}{K_a}\right) \tag{3.27}$$

The above equation can be used to estimate the depth of tensional zone under various suction stress or matric suction conditions which varies with time and depth.

3.3.3.2 Passive earth pressure

Passive earth pressure mobilized in situations such as a soil mass in front of a failing retaining wall or an expansive soil mass behind a retaining wall (Lu and Likos 2004). In passive earth pressure the horizontal pressure is usually greater than the vertical stress induced by soil weight. Regarding the Mohr Coulomb criterion, the state of failure occurs when the horizontal stress develops to a level in which the combination of normal and shear stress exceeds the failure envelope. The fundamental difference in passive and active state of failure is the direction of principal stresses. Despite of active stress, the horizontal effective stress is the maximum principal stress and the vertical overburden stress is the minimum principal stress. Employing the above mentioned idea allows one to define the passive lateral pressure as:

$$\sigma_h' = \sigma_v' K_p + 2c'\sqrt{K_p} \tag{3.28}$$

where K_p is the coefficient of Rankin's passive pressure defined as:

$$K_p = \tan^2\left(\frac{\pi}{4} + \frac{\phi'}{2}\right) \tag{3.29}$$

The extension of Eq. (3.28) for unsaturated soils is accomplished by introducing the suction stress as a third stress component:

$$(\sigma_h - u_a) = (\sigma_v - u_a)K_p + 2c'\sqrt{K_p} + (1 - K_p)\sigma^s \tag{3.30}$$

Subsequently, the unsaturated Rankin's passive coefficient is derived by dividing the right hand side of Eq. (3.30) over vertical effective stress:

$$K_{pu} = \frac{\sigma_h - u_a}{\sigma_v - u_a} = K_p + \frac{2c'\sqrt{K_p}}{\sigma_v - u_a} - \frac{(K_p - 1)\sigma^s}{\sigma_v - u_a} \tag{3.31}$$

Combination of three terms shapes the passive lateral earth pressure for partially saturated soils. The first two terms are well-known parameters from classical Rankine's theory. The third term introduced by Lu and Likos (2004) expresses the nonlinear behavior of suction stress in spatial variation. Regardless of the active earth pressure, all three terms contribute to compressive earth pressure. Figure (3.3) represents the schematic variation of passive earth pressure in the depth of a retaining structure for all three terms. The trend for the effect of overburden stress, mobilized cohesion, and suction stress are constant, linear, and nonlinear in the soil depth.

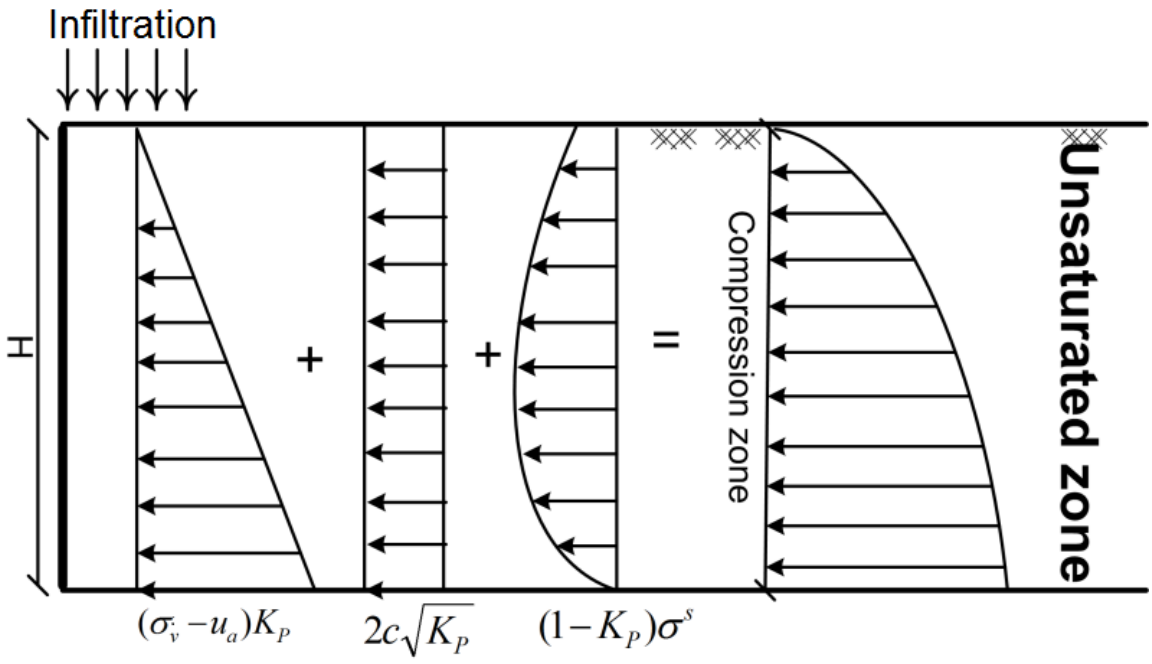

Figure 3.3 Tension and compression stresses under transient flow in passive mode of failure

3.4 Results and discussion

The aforementioned formulations can be employed to evaluate the role and impact of different parameters on active and passive earth pressure profiles under transient flow. In this section we investigate the effect of hydrological and mechanical properties of different soils on the pore water pressure profiles, which include pressure head, suction stress and lateral earth pressures in different time intervals. A numerical model is developed using numerical software COMSOL to solve the one dimensional coupled hydro-mechanical governing equation for infiltration (i.e., Eq. 3.21) and then the results are compared with the uncoupled governing equations for infiltration (i.e., Eq. 3.22) for different hypothetical soil types. A thickness of 5.0 m is assumed for the simulation of coupled/uncoupled models and also for the active/passive pressure profiles

for all soil types. The boundary conditions are set at lower and upper boundaries. The lower boundary of the model is considered to be at the water table where the pore water pressure is 0. Whereas, a constant flux is applied on the top boundary (infiltration). The results obtained from the numerical model include the pressure head profiles as a function of depth at different time intervals for different soils. The evaluated outputs are used to study the lateral earth pressure profiles. Table 3.1 illustrates the hydrological and mechanical properties of soils considered in this study. The mechanical properties of the investigated soils (ϕ',c',and γ(unit weight)) are constant but the hydrological properties of soils (S_e, K, and θ) vary in both depth and time. In the all cases Gardner's equations (i.e., Eq.(3.3) and Eq.(3.4)) are used to describe SWRC and subsequently, the suction stress. The rate of infiltration (Q/K_s) is considered constant and is equal to 1.0 in all cases. The initial negative pore water pressure is assumed to be hydrostatic and the effect of atmospheric pressure is neglected ($u_a = 0$) for all cases. The representation of illustrative examples begins with the analysis of different pressure profiles for fine sands and is followed by silt. In this sequence the probability of organic content presence in the soils increases whereas, the hydraulic conductivity and the parameter α decrease.

Table 3.1 Hydrological and Mechanical properties of hypothetical Soils

Soil Type	$\boldsymbol{\alpha}$ $(\boldsymbol{m^{-1}})$	$\boldsymbol{K_s}$ $(\boldsymbol{ms^{-1}})$	$\boldsymbol{\theta_s}$	$\boldsymbol{\theta_r}$	$\boldsymbol{E}$ $(\boldsymbol{kPa})$	$\boldsymbol{c'}$ $(\boldsymbol{kPa})$	$\boldsymbol{\phi'}$ $(\boldsymbol{degree})$	$\boldsymbol{\gamma}$ $\left(\boldsymbol{kNm^{-3}}\right)$
Fine sand	0.7	$5.0e^{-6}$	0.41	0.05	3×10^4	0.0	40	18
Silt	0.5	$9.0e^{-7}$	0.45	0.10	5×10^3	1.7	30	19

3.4.1 Profiles of lateral earth pressures in fine sand

A theoretical example of fine sand from Lu and Godt (2013) is considered to study the effect of transient flow on the different pressure profiles. The profiles of the pressure head, the suction stress, and the active stress are studied in both coupled and uncoupled scenarios. The profiles of the pressure head, the suction stress, and the active stress show an increasing trend whereas the passive earth pressure shows a decreasing trend with time. Figure 3.4 shows the variation of above mentioned terms in 10 hrs simulation, with the time sequence of t = 2, 4, and 10 hrs. The time for dissipation of negative pore pressure increases with increase in fineness of the soil. The results for coupled analysis are shown as red solid line; whereas the blue dashed line represents the uncoupled analysis. Figure 3.4(a) shows considerable variations in pore pressure for coupled and uncoupled analysis in pre-selected time intervals. It shows that there is a subsequent difference between the coupled and uncoupled scenarios, which results in the pressure head in uncoupled analysis, dissipates more rapidly than the coupled analysis. Consequently, it leads to subsequent differences in suction stress (Figure 3.4(b)). For example, the suction stress in coupled analysis near the surface changes from about $-4.7\ kPa^{-1}$ at $t\ =\ 2\ hrs$ to almost $-1.1\ kPa^{-1}$ at $t\ =\ 10\ hrs$. Similarly, behavior for the suction stress can be seen in the uncoupled analysis. This considerable difference in suction stress near the surface highlights the necessity of accurate study of changes in active/passive lateral earth pressure in fine sand under transient flow. The active earth pressure increases with time while its trend alters from nonlinear distribution in depth in early stages of infiltration to a straight line when the negative pore pressure has dissipated in soil mass. Although the cohesion is zero in this material, the negative earth pressure

near the surface is noticeable (Figure 3.4(c)). This condition warrants the monitoring of tension cracks in early stage of infiltration even in fine sands without cohesion. Figure 3.4(d) shows a slight nonlinear trend for passive earth pressure distribution in soil at $t =$ 2 hrs. However, despite of active earth pressure, the magnitude of passive earth pressure decreases within time and its behavior changes from nonlinear to linear.

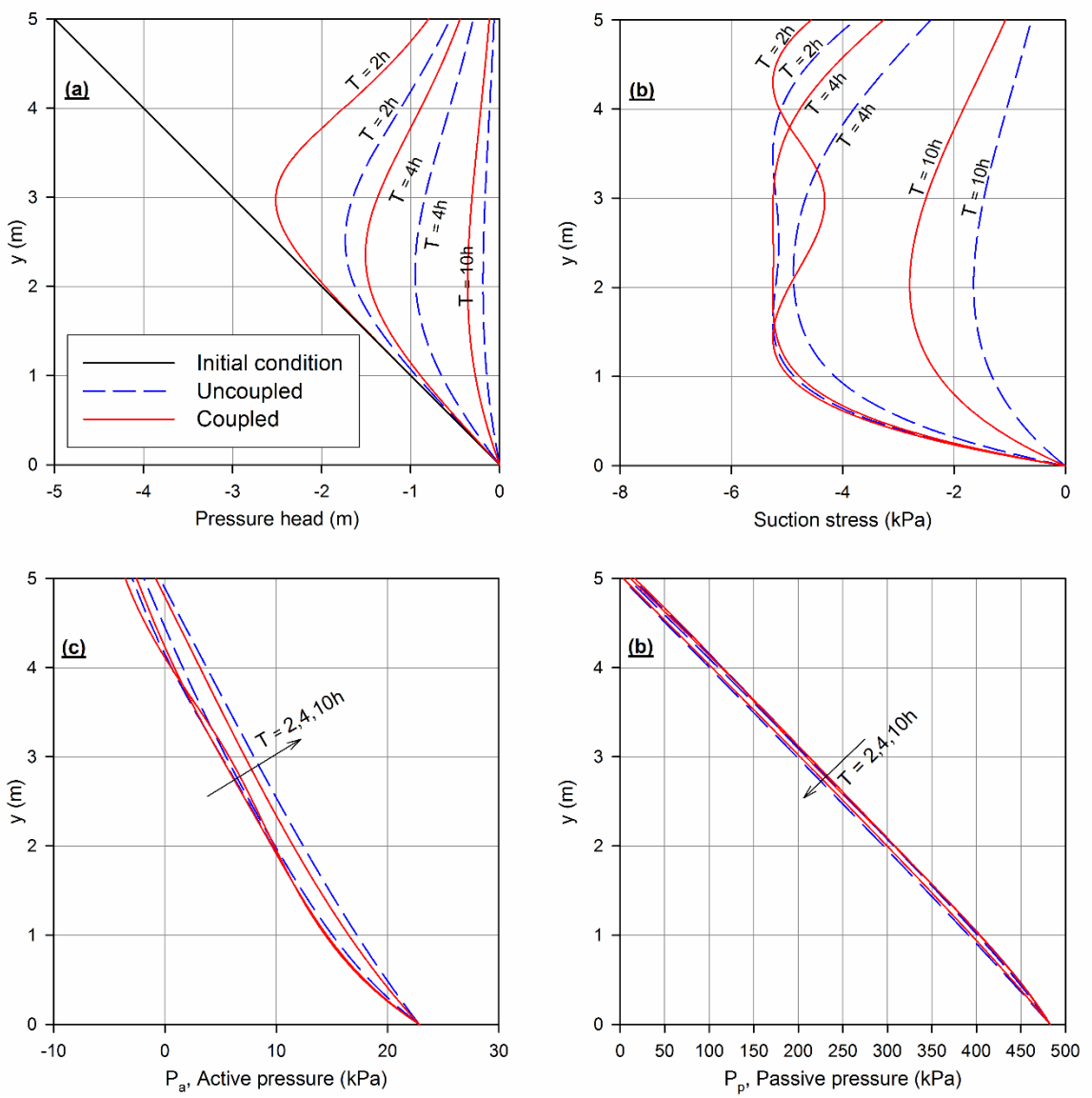

Figure 3.4 Variation in different pressure profiles due to changes in hydrological properties of fine sand

a) Pressure head as a function of depth. b) Suction stress versus depth. c) Dynamic active earth pressure (P_a) with respect to time. d) Dynamic passive earth pressure (P_p) with respect to time

Since the effect of suction stress is significant in fine sands, Eq. (3.20) is used to specify the tension zone. Figure 3.5 depicts the compression and tension zone for both coupled and uncoupled analysis while active earth pressure is considered. To highlight

the importance of analysis of active earth pressure under transient flow, different time intervals are chosen corresponding to the compression and tension zones. The first scenario considers the interaction of compression and tension stresses at $t = 2$ hrs and the second scenario attempts to analysis the conditions at $t = 10$ hrs. It is obvious that the first scenario includes larger suction stress which leads to producing considerable tension stress while in the second scenario almost steady-state condition governs the system in which the suction stress is much less than first case and compression stress is generated in this case.

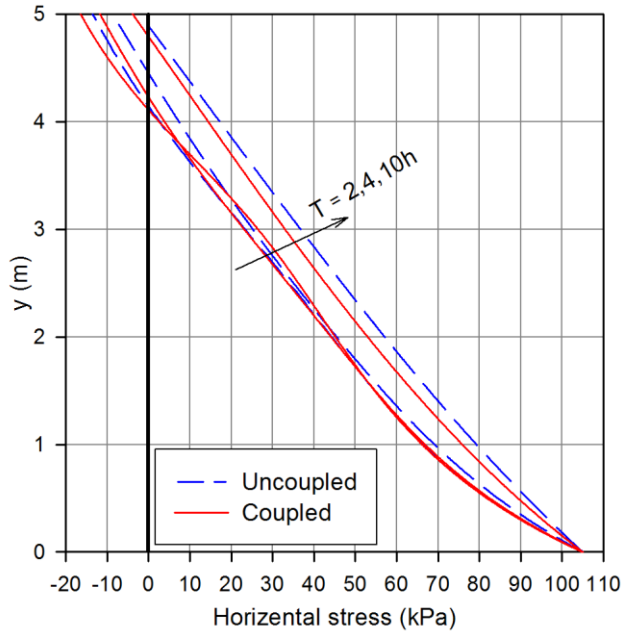

Figure 3.5 Tension and compression zones for transient and semi steady-state conditions

We know from classical soil mechanics that the soil mass in tension zone does not contribute to soil strength and the soil body in tension zone should be treated as

surcharge. This statement emphases the analysis of retaining walls in early stage of infiltration in which the risk of failure is pronounced in comparison with the steady-state cases.

3.4.2 Profiles of lateral earth pressure in silt

It is common in engineering problems to face fine grain soils (i.e., silt and clay) in excavations or trench formations. This example represents the coupled and uncoupled analysis along with the active/passive, tension and compression stresses under transient infiltration in a 5m thick unsaturated layer of silt. The same initial and boundary conditions as considered in previous example are implemented in this problem. The analysis is done for a duration of 20 hours with pre-selected time intervals of $t = 5,10$ and 20 hrs. The maximum negative pressure head for coupled is about -3.4 m near the depth of around 3.8 m and for uncoupled maximum pore pressure is about -2.6 m near the depth of 3.2 m at t = 5 hrs. However, the corresponding pore pressures of coupled and uncoupled analysis at the surface is about -1.8 m and -1.3 m respectively. These conditions lead to higher suction stress at the corresponding locations (Figure 3.6 (a) and (b)). Although, the behavior of the suction stress profile in coupled analysis for 5 hrs and10 hrs is little complex as there is comparatively significant increase in negative suction stress. However, as time goes by, the suction stress starts to increase. A considerable difference can be observed between the coupled and uncoupled analysis of suction stress at t = 20 hrs. The two points which show the higher negative suction stress are considered as they contribute to both active and passive earth pressure generation. In the active earth pressure scenario the probability of tension cracks formation is high near the soil surface especially in the absence of surcharge. It is necessary to consider the

effect of cohesion for fine soils when this parameter compounds with suction stress and intensifies the probability of tension cracks formation within tension zone. Figure 3.6 (c) depicts the impact of suction stress on the formation of tension zone at the beginning of simulation. The magnitude of active earth pressure for both coupled and uncoupled analysis is -6 kPa^{-1} at t = 5 hrs and gradually tends towards zero at time goes by near the soil surface. However, the results do not show much difference between the coupled and uncoupled active earth pressure profiles. The analysis of passive earth pressure in this problem illustrates that the trend for passive stress is not sensitive to time (Figure 3.6 (d)).

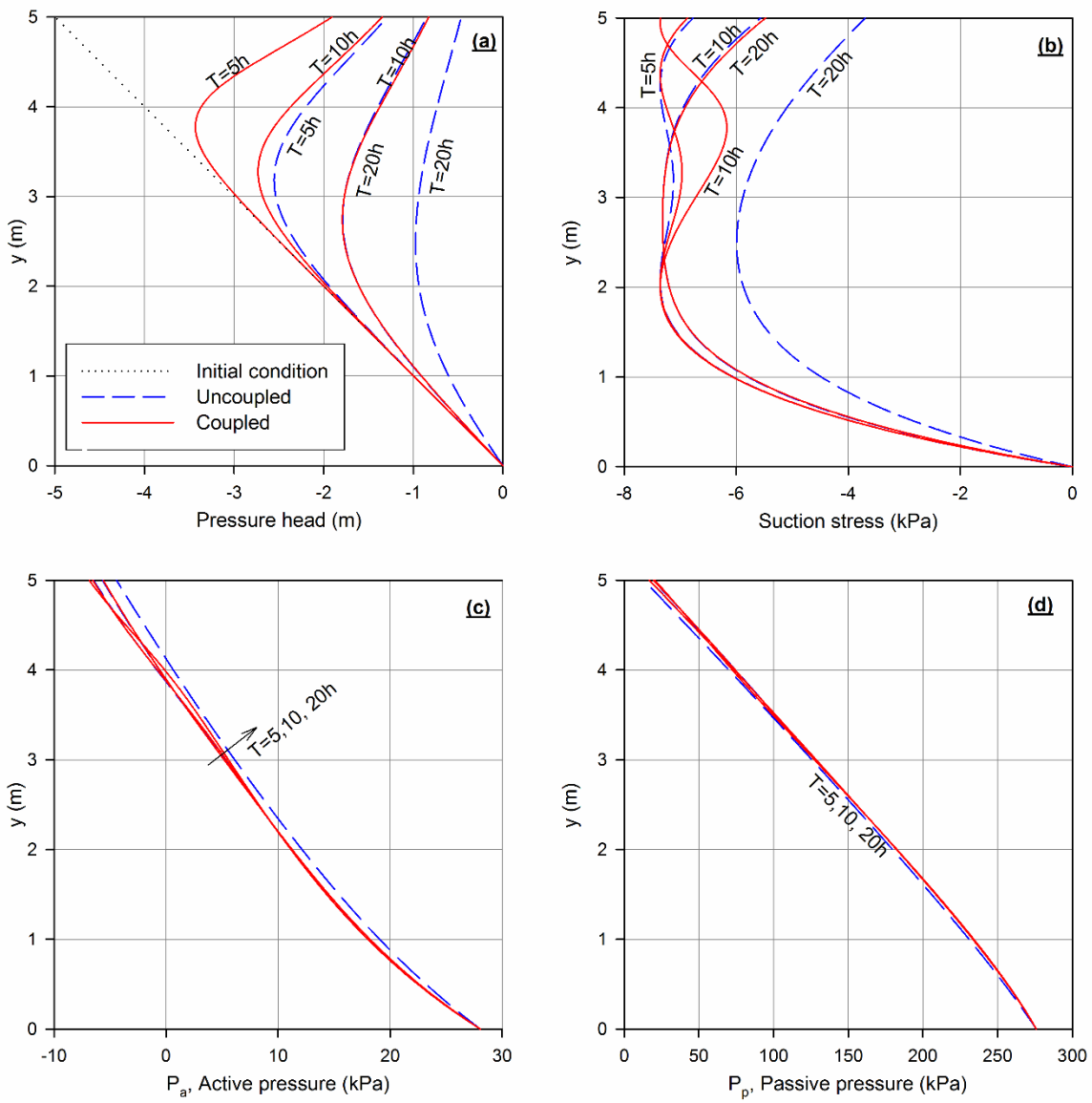

Figure 3.6 Variation in different pressure profiles due to changes in hydrological properties of silt

a) Pressure head as a function of depth. b) Suction stress versus depth. c) Dynamic active earth pressure (P_a) with respect to time. d) Dynamic passive earth pressure (P_p) with respect to time

Figure 3.7 represents the depth of tension zone for the time intervals of t = 5, 10 and 20 hrs. In this case also the importance of monitoring the tension zone in early ages of infiltration is signified by the outcomes of analysis. It is noticeable that by increasing

the time the analysis shows the low impact of tension stress in the soil mass. For example the depth of tension zone is more than 1 m in the analysis of active earth pressure for both coupled and uncoupled analysis at t = 5 hrs. In addition, the distribution of active earth pressure along the soil depth in the initial stages is nonlinear. However, as the time goes by, the trend changes from a nonlinear to linear trend with respect to time as can be seen for t = 20 hrs uncoupled analysis.

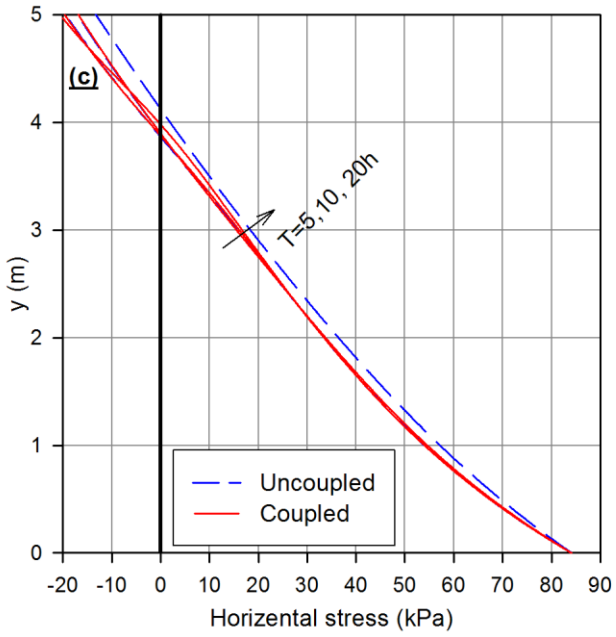

Figure 3.7 Tension versus compression zones for transient flow in t = 5, 10 and 20 hrs

CHAPTER IV

SUMMARY AND CONCLUSIONS

4.1 Summary and conclusion of work accomplished for empirical equivalence of the fitting parameters of soil water retention models

In this work an empirical correlation was proposed to convert FX's fitting parameters to the BC parameters and consequently generate the retention curve for BC using the converted parameters. Several approaches for parameter convergence of BC with FX were investigated including capillary drive, capillary length, and shape index but due to the incompetence of the FX function, analytical closed form solutions cannot be obtained for the equivalence with BC. Therefore, an empirical approach was used for the convergence of BC and FX. A constrained non-linear optimization method was used to evaluate the fitting parameters of each retention function and subsequently generate the SWRC's for BC and FX. Moreover, another retention curve was generated for BC using the proposed equation to convert FX parameters (m, n) to BC parameter (λ). The fitting parameters of FX were compared with fitting parameters of BC to investigate any direct correlation. The results of the comparison between estimated and optimized BC parameter (λ) indicated that the suggested co-relation provides reasonably good evaluation of BC parameter (λ). The comparison of the SWRC's for BC, FX and for BC from FX (BC-FX) with the measured retention data also showed a good agreement with the proposed correlation. Therefore, it can be concluded that the proposed BC-FX is in correspondence with the actual BC retention curve and to overcome the problems of

direct fitting of BC with measured data, FX parameters can be used to generate the BC retention curve.

4.2 Summary and conclusion of work accomplished for coupled and uncoupled earth pressure profiles in unsaturated soils under transient flow

The purpose of this work was to find the changes in lateral earth pressure based coupled/uncoupled transient unsaturated infiltration and deformation in the soil body. Variations in the degree of saturation in transient flow lead to the wetting front propagation. Subsequently, matric suction, suction stress, and effective stress significantly vary in time. Extension of Rankin's theory based on matric suction and effective stress shows dynamic changes in active/passive pressure in time. In order to find the effective stress, coupled and uncoupled unsaturated transient seepage could be considered simultaneously with soil body deformation. The analysis results show that the time for dissipation of negative pore water pressure is longer in the coupled formulation in comparison with uncoupled simulation. The dissipation time also affects the dynamics of matric suction variation and eventually the active/passive lateral earth pressure. In general the active earth pressure is more sensitive to wetting front propagation and active pressure increases as negative pore water pressure dissipates while passive lateral earth pressure remains almost unchanged for both fine sand and silt.

In general, suction due to the negative pore water pressure shows formation of tension zones even in soils without cohesion (fine sand). Tension zones are vulnerable of forming tension cracks and soil strength is negligible in these zones. This statement is critical for structures where formation of tension zones have not been considered for their performance. Finally, for a combination of a short-duration heavy rain and high initial

suction, the performance of existing structures near trenches, cutoff walls and excavations could be highly affected by variable lateral earth pressure.

4.3 Recommendations for future work

As for the first part of this work, a more robust method can be developed for the equivalence of the complex retention models (non-linear functions) to simpler retention models. The main reason for this is to decrease the number of fitting parameters in addition to the implementation of the analytical approaches to yield more practical results. The analytical solutions for the simpler retentions functions like BC, can be easily developed and the solutions can be used in some other studies where the implementation of the complex retention functions is not practical such as for the coupled analysis of infiltration and deformation in unsaturated soils. Whereas, the retention functions proposed by van Genuchten (1980), Fredlund and Xing (1994) and more recently by Lu (2016) are more continuous and provide better fit than the simpler models like Gardner (1958), Brooks and Corey (1964). Therefore, by developing a robust conversion approach the properties of more accurate models can be converted to simpler retention models and can be employed to analytical studies easily.

For the second part of this research, the numerical results from coupled and uncoupled simulations reveal that the coupling of seepage and deformation strongly controls the propagation of wetting front, matric suction, effective stress, and finally, lateral earth pressure. In comparison with uncoupled analysis, this study recommends that the coupling of seepage and deformation should be taken into account when the rainfall infiltration considered upon the unsaturated porous medium. Specifically, for a combination of a short-duration heavy rain and high initial suction, the performance of

existing structures near trenches, cutoff walls and excavations could be highly affected by variable lateral earth pressure. Moreover, one-dimensional transient flow study of coupled and uncoupled earth pressure profiles in unsaturated soils can be extended to two dimensional coupled hydro-mechanical model which would provide more realistic and practical results. The implementation of more accurate and continuous SWR functions or the correlated complex functions to the simpler ones in the coupled/uncoupled model can be done. Other than the numerical models, analytical approaches can be adopted to solve coupled/uncoupled problems.

REFERENCES

Alonso EE, Lloret A, Gens A, Battle F (1989) A new approach for the prediction of long term heave. In: Proceedings of the 12th ICSMFE, Rio de Janeiro, vol 1, pp 571–574

Assouline, S., and D. Tartakovsky (2001), Unsaturated hydraulic conductivity function based on a soil fragmentation process, Water Resour. Res., 37(5), 1309–1312, doi:10.1029/2000WR900332.

Bishop, A. W. (1959). "The principle of effective stress." Tek Ukeblad, 106(39), 859–863.

Blake, J. R., Renaud, J. P., Anderson, M. G., & Hencher, S. R. (2003). Prediction of rainfall-induced transient water pressure head behind a retaining wall using a high-resolution finite element model. Comput and Geotech, 30(6), 431-442.

Brooks, R. H., and a T. Corey (1964), Hydraulic properties of porous media, Hydrol Pap Fort Collins CO Colo State Univ, 3(3), 27 pgs, doi:citeulike-article-id:711012.

Burdine, N. T. (1953), Relative permeability calculations from pore size distribution data, J. Pet. Technol., 5(3), 71–78, doi:10.2118/225-G.

Chen, F.H. (1988). Foundations on expansive soils, Elsevier, New York.

Cho SE, Lee SR (2001) Instability of unsaturated soil slopes due to infiltration. Comput Geotech 28:185–208

Cihan, A., J. S. Tyner, and E. Perfect (2009), Predicting relative permeability from water retention: A direct approach based on fractal geometry, Water Resour. Res., 45(4), 1–8, doi:10.1029/2008WR007038.

Eisenhauer, J.G. (2003). "Regression through the Origin," Teaching Statistics, 25(3), 76-80.

Fredlund, D. G., and Morgenstern, N. R. (1977). "Stress state variables for unsaturated soils." J. Geotech. Engrg. Div., 103(5), 447–466.

Fredlund, D. G., and Rahardjo, H. (1993). Soil mechanics for unsaturated soils, Wiley, New York.

Fredlund, D. G., A. Xing, and S. Huang (1994), Predicting the permeability function for unsaturated soils using the soil-water characteristic curve, Can. Geotech. J., 31(4), 533–546, doi:10.1139/t94-062.

Fredlund, D. G., and A. Xing (1994), Equations for the soil-water characteristic curve, Can. Geotech. J., 31(3), 1026–1026, doi:10.1139/t94-120.

Fredlund, M. D., G. W. Wilson, and D. G. Fredlund (2002), Use of the grain-size distribution for estimation of the soil-water characteristic curve, *Can. Geotech. J.*, *39*, 1103–1117, doi:10.1139/t02-049.

Damiano, E., and Mercogliano, P. (2013). "Potential effects of climate change on slope stability in unsaturated pyroclastic soils." Landslide science and practice: Volume 4: Global environmental change, C. Margottini, P. Canuti,

Day, R.W. (1994). "Swell – shrink behaviour of expansive compacted clay, Journal of Geotechnical Engineering," ASCE, Vol.120, No.3, 618-623.

Gallage, C., J. Kodikara, and T. Uchimura (2013), Laboratory measurement of hydraulic conductivity functions of two unsaturated sandy soils during drying and wetting processes, Soils Found., 53(3), 417–430, doi:10.1016/j.sandf.2013.04.004.

Gardner, W. R. (1958), Some steady state-solutions of the unsaturated moisture flow equation with application to evaporation from a water table., *Soil Sci. Soc. Am. J.*, *85*(4), 228.232.

Ghezzehei, T. A., T. J. Kneafsey, and G. W. Su (2007), Correspondence of the Gardner and van Genuchten-Mualem relative permeability function parameters, Water Resour. Res., 43(10), 1–7, doi:10.1029/2006WR005339.

Haverkamp, R., F. J. Leij, C. Fuentes, F. Zatarain, P. J. Ross, A. Sciortino, F. J. Leij, C. Fuentes, A. Sciortino, and P. J. Ross (2005), Soil Water Retention: I. Introduction of a Shape Index, Soil Sci. Soc. Am. J., 69(6), 1881, doi:10.2136/sssaj2004.0225.

Kosugi, K.I., Hopmans, J.W. and Dane, J.H., 2002. 3. 3. 4 Parametric models. Methods of Soil Analysis: Part 4 Physical Methods, (methodsofsoilan4), pp.728-757.

Lamara, M., and Z. Derriche (2008), Prediction of unsaturated hydraulic properties of dune sand on drying and wetting paths, Electron. J. Geotech. Eng., 13 B.

Leij, F. J., R. Haverkamp, C. Fuentes, F. Zatarain, P. J. Ross, A. Sciortino, F. J. Leij, C. Fuentes, A. Sciortino, and P. J. Ross (2005), Soil Water Retention: II. Derivation and Application of Shape Index, Soil Sci. Soc. Am. J., 69(6), 1881, doi:10.2136/sssaj2004.0225.

Leij, F. J., Schaap, M. G., & Arya, L. M. (2002). 3.6. 3 Indirect Methods. Methods of Soil Analysis: Part 4 Physical Methods, (methodsofsoilan4), 1009-1045.

Leij, F., W. Alves, M. Van Genuchten, and J. Williams (1996), The UNSODA Unsaturated Soil Hydraulic Database; User's Manual, Version 1.0, Rep. EPA/600/R-96, (August), 113.

Lenhard, R. J., J. C. Parker, and S. Mishra (1989), On the correspondence between Brooks-Corey and van Genuchten models., J. Irrig. Drain. Eng., 115(4), 744–751.

Leong, E. C., and H. Rahardjo (1997), REVIEW OF SOIL-WATER CHARACTERISTIC CURVE EQUATIONS, *J. Geotech. Geoenvironmental Eng.*, *123*(December), 1106–1117.

Godt, J. W., Baum, R., and Lu, N. (2009). "Land sliding in partially saturated materials." Geophys. Res. Lett., 36(2), L02403.

Godt, J. W., Şener Kaya, B., Lu, N., & Baum, R. L. (2012). Stability of infinite slopes under transient partially saturated seepage conditions. Water Resour. Res., 48(5).

Hong, G. T. (2008). "Earth pressures and deformations in civil infrastructure in expansive soils." Ph.D. dissertation, Texas A&M Univ., College Station, TX.

Jones, D.E. and Holtz, W.G. (1973). "Expansive soils - the hidden disaster." Civil Engineering, 43(8), 49–51.

Kim JM (2000) A fully coupled finite element analysis of water table fluctuation and land deformation in partially saturated soils due to surface loading. Int J Numer Meth Eng 49:1101–1119

Kim, S. K., and Borden, R. H. (2013). "Numerical simulation of MSE wall behavior induced by surface-water infiltration." J. Geotech. Geoenviron. Eng., 10.1061/(ASCE)GT.1943-5606.0000927, 2110–2124.

Koerner, R. M., and Koerner, G. R. (2013). "A data base, statistics and recommendations regarding 171 failed geosynthetic reinforced mechanically stabilized earth (MSE) walls." Geotext. Geomembr., 40, 20–27.

Liang,W., Zhao, J., Li, Y., Zhang, C.,Wang, S. (2012). "Unified solution of Coulomb's active earth pressure for unsaturated soils without crack." Appl. Mech. Mater., 170–173, 755–761.

Lloret A, Gens A, Batlle F, Alonso EE (1987) Flow and deformation analysis of partially saturated soils. In: Proceedings of the 9th European conference on soil mechanics and foundation engineering, Dublin, vol 2, pp 565–568

Lu, N. (2008). "Is matric suction a stress variable?" J. Geotech. Geoenviron. Eng., 10.1061/(ASCE)1090-0241(2008)134:7(899), 899 905.

Lu, N., and Godt, J. W. (2013). Hillslope hydrology and stability. Cambridge University Press.

Lu, N., and Likos, W. J. (2006). "Suction stress characteristic curve for unsaturated soil." J. Geotech. Geoenviron. Eng., 10.1061/(ASCE) 1090-0241(2006)132:2(131), 131–142.

Lu, N., Godt, J. W., and Wu, D. T. (2010). "A closed-form equation for effective stress in unsaturated soil." Water Resour. Res., 46(5), W05515.

Lu. N., Likos, W., (2004). "Unsaturated Soil Mechanics." John Wiley & Sons, Inc., Hoboken, New Jersey.

Lu, N., and F. Asce (2016), Generalized Soil Water Retention Equation for Adsorption and Capillarity, J. Geotech. Geoenvironmental Eng., doi:10.1061/(ASCE)GT.1943-5606.0001524.

Ma, Q., J. E. Hook, and L. R. Ahuja (1999), Influence of three-parameter conversion methods between van Genuchten and Brooks-Corey functions on soil hydraulic properties and water-balance predictions, Water Resour. Res., 35(8), 2571–2578.

Milly, P. C. D. (1987), Estimation of Brooks-Corey Parameters from water retention data, Water Resour. Res., 23(6), 1085–1089.

Morel-Seytoux, H. J., P. D. Meyer, M. Nachabe, J. Touma, M. T. van Genuchten, and R. J. Lenhard (1996), Parameter equivalence for the Brooks-corey and van Genutchen soil characteristics: Preserving the effective capillary drive, Am. Geophys. Union, 32(5), 1251–1258.

Mualem, Y. (1976), A new model for predicting the hydraulic conductivity of unsaturated porous media, Water Resour. Res., 12(3), 513–522, doi:10.1029/WR012i003p00513.

Nelson, J.D. and Miller, J. D. (1992). "Expansive Soils, Problems and Practice in Foundation and Pavement Engineering." Wiley Press, New York.

Philip, J. R. (1985), Reply to "Comments on Steady Infiltration from Spherical Cacvities," , 49.

Phoon, K.-K., A. Santoso, and S.-T. Quek (2010), Probabilistic Analysis of Soil-Water Characteristic Curves, J. Geotech. Geoenvironmental Eng., 136(March), 445–455, doi:10.1061/(ASCE)GT.1943-5606.0000222.

Pufahl, D., Fredlund, D., and Rahardjo, H. (1982). "Lateral earth pressures in expansive clay soils." Can. Geotech. J., 20(2), 228–241.

Puppala, A.J. and Cerato, A. (2009). "Heave distress problems in chemically-treated sulfate-laden materials." Geo-Strata, 10(2), 28–30, 32.

Rahardjo, H., and E. G. Leong (1997), *Soil water characteristic curve and flux boundary problems*. Rahardjo, H., Rezaur, R. B., Leong, E. C., Alonso, E. E., Lloret, A., and Gens, A. (2008). "Monitoring and modeling of slope response to climatic changes." Proc., 10th Int. Symp. on Landslides and Engineered Slopes, Z. Chen, J.-M. Zhang, K. Ho, F.-Q. Wu, and Z.-K. Li, eds.,

Ravichandran N (2009) Fully coupled finite element model for dynamics of partially saturated soils. Soil Dyn Earthq Eng 29:1294–1304

Rucker, D. F., A. W. Warrick, and T. P. A. Ferr?? (2005), Parameter equivalence for the Gardner and van Genuchten soil hydraulic conductivity functions for steady vertical flow with inclusions, Adv. Water Resour., 28(7), 689–699, doi:10.1016/j.advwatres.2005.01.004.

Ruwaih, I.A., (1987). "Experiences with expansive soils in Saudi Arabia." Proceedings of the 6th International Conference on Expansive Soils, New Delhi, India, pp. 317–322.

Seki, K. (2007) SWRC fit - A nonlinear fitting program with a water retention curve for soils having unimodal and bimodal pore structure. Hydrol. Earth Syst. Sci. Discuss., 4: 407-437.doi:10.5194/hessd-4-407-2007

Srivastava, R., & Yeh, T. C. J. (1991). Analytical solutions for one-dimensional, transient infiltration toward the water table in homogeneous and layered soils. Water Resour. Res, 27(5), 753-762.

Tavakkoli, N., and Vanapelli, S. K. (2011). "Rational approach for the design of retaining structures using the mechanics of unsaturated soils." Proc., 2011 Pan-American CGS Geotechnical Conf., Canadian Geotechnical Society, Richmond, BC, Canada.

Thomas, H. R., and Y. He (1995), Analysis of coupled heat, moisture and air transfer in a deformable unsaturated soil, Geotechnique, 45(4), 677–689.

Timlin, D. J., L. R. Ahuja, Y. Pachepsky, R. D. Williams, D. Gimenez, and W. Rawls (1999), Use of Brooks-Corey Parameters to Improve Estimates of Saturated Conductivity from Effective Porosity, *Soil Sci. Soc. Am. J.*, *63*(October), 1086, doi:10.2136/sssaj1999.6351086x.

van Genuchten, M. T. (1980), A Closed-form Equation for Predicting the Hydraulic Conductivity of Unsaturated Soils., *Soil Sci. Soc. Am. J.*, *44*(5), 892–898.

van Genuchten, M. T., and D. R. Nielsen (1985), On describing and predicting the hydraulic properties of unsaturated soils, Ann. Geophys., 3(5), 615–628, doi:10.1111/j.1468-2494.2010.00560.x.

van Genuchten, M. T., F. J. Leij, and S. R. Yates (1991), The RETC code for quantifying the hydraulic functions of unsaturated soils, United States Environ. Reseach Lab., (December), 93, doi:10.1002/9781118616871.

Vahedifard, F. and Robinson, J. (2015). "Unified Method for Estimating the Ultimate Bearing Capacity of Shallow Foundations in Variably Saturated Soils under Steady Flow." J. Geotech. Geoenviron. Eng., 10.1061/(ASCE)GT.1943-5606.0001445 , 04015095.

Vahedifard, F., B. A. Leshchinsky, K. Mortezaei, and N. Lu (2015), Active Earth Pressures for Unsaturated Retaining Structures, J. Geotech. Geoenvironmental Eng., 141(11), 1–11, doi:10.1061/(ASCE)GT.1943-5606.

Vahedifard, F., D. Leshchinsky, K. Mortezaei, and N. Lu (2016a), Effective Stress-Based Limit-Equilibrium Analysis for Homogeneous Unsaturated Slopes, Int. J. Geomech., 1–10, doi:10.1061/(ASCE)GM.1943-5622.0000554.

Vahedifard, F., K. Mortezaei, B. A. Leshchinsky, D. Leshchinsky, and N. Lu (2016b), Transportation Geotechnics Role of suction stress on service state behavior of geosynthetic- reinforced soil structures, Transp. Geotech., doi:10.1016/j.trgeo.2016.02.002.

Valentine, R. J. (2013). “An assessment of the factors that contribute to the poor performance of geosynthetic-reinforced earth retaining walls.” Proc., Int. Symp. on Design and Practice of Geosynthetic-Reinforced Soil Structures, H. I. Ling, G. Gottardi, D. Cazzuffi, J. Han, and F. Tatsuoka, eds., DEStech, Lancaster, PA, 318–327.

Vanapalli, S. K., Fredlund, D. E., Pufahl, D. E., and Clifton, A. W. (1996). “Model for the prediction of shear strength with respect to soil suction.” Can. Geotech. J., 33(3), 379–392.

Vo, T., & Russell, A. R. (2014). Slip line theory applied to a retaining wall–unsaturated soil interaction problem. Comput and Geotech, 55, 416-428.

Vanapalli, S. K., & Fredlund, D. G. (2000). Comparison of different procedures to predict unsaturated soil shear strength. Geotechnical Special Publication, 195-209.

Vo, T., Taiebat, H., & Russell, A. R. (2016). Interaction of a rotating rigid retaining wall with an unsaturated soil in experiments. Géotechnique, 1-12.

Warrick, A. (1995), Correspondence of Hydraulic Functions for Unsaturated Soils., Soil Sci. Soc. Am. J., 59(2), 292–299.

Wu, L. Z., and L. M. Zhang (2009), Analytical solution to 1D coupled water infiltration and deformation in unsaturated soils, Int. J. Numer. Anal. Methods Geomech., 33(July), 773–790, doi:10.1002/nag.742.

Wu, L. Z., L. M. Zhang, and R. Q. Huang (2011), Analytical solution to 1D coupled water infiltration and deformation in two-layer unsaturated soils, Int. J. Numer. Anal. Methods Geomech., (May 2011), 798–816, doi:10.1002/nag.

Wu, L. Z., A. P. S. Selvadurai, and R. Q. Huang (2013), Two-Dimensional Coupled Hydromechanical Modeling of Water Infiltration into a Transversely Isotropic Unsaturated Soil Region, Vadose Zo. J., 12, 0, doi:10.2136/vzj2013.04.0072.

Wu, L. Z., L. M. Zhang, and X. Li (2015), One-Dimensional Coupled Infiltration and Deformation in Unsaturated Soils Subjected to Varying Rainfall.

Wu, L. Z., G. G. Liu, L. C. Wang, L. M. Zhang, B. E. Li, and B. Li (2016), Numerical analysis of 1D coupled infiltration and deformation in layered unsaturated porous medium, Environ. Earth Sci., (October), doi:10.1007/s12665-016-5579-4.

Yeh, T. C. J. (1989). One-dimensional steady state infiltration in heterogeneous soils. Water Resour. Res. 25(10), 2149-2158.

Yelti, N. (2011). Analysis and design of soil nail walls in high plasicity clays. The University of Texas at San Antonio.

Yoo, C., and Jung, H. (2006). "Case history of geosynthetic reinforced segmental retaining wall failure." J. Geotech. Geoenviron. Eng., 10.1061/(ASCE)1090-0241(2006)132:12(1538), 1538–1548.

Zhang, C., Zhao, J., Zhang, Q., and Xu, F. (2010). "Unified solutions for unsaturated soil shear strength and active earth pressure." Experimental and applied modeling of unsaturated soils, Geotechnical Special Publication No. 202, L. R. Hoyos, X. Zhang, and A. J. Puppala, eds., ASCE, Reston, VA, 218–224.

Zhang LL, Zhang J, Zhang LM, Tang WH (2011) Stability analysis of rainfall-induced slope failure: a review. P I Civil Eng-Geotec 164:299–316

Zhan, T. L. T., G. W. Jia, Y. M. Chen, D. G. Fredlund, and H. Li (2013), An analytical solution for rainfall infilration into an unsaturated infinite slope and its application to slope stability analysis, Int. J. Numer. Anal. Methods Geomech., doi:10.1002/nag.2106.

Zhang, G. R., Y. J. Qian, Z. C. Wang, and B. Zhao (2014), Analysis of rainfall infiltration law in unsaturated soil slope, Sci. World J., 2014, 1–8, doi:10.1155/2014/567250.

Zhao HF, Zhang LM (2014) Instability of saturated and unsaturated coarse granular soils. J Geotech Geoenviron 140:25–35